

AGN Jet Workshop 2020

"Active Galactic Nucleus Jets in the Event Horizon Telescope Era"

Hosted by Tohoku University
Aoba Science Hall in Science Complex C, Aobayama Campus, Tohoku University, Sendai

January 20 (Mon) - 22 (Wed) : Workshop

January 23 (Thu) : VLBI proposal writing

****The proposal writing is intended for EHTC (internal and external) members only****

	Top	Practical Info	Registration	Participants	Program	
--	---------------------	--------------------------------	------------------------------	------------------------------	-------------------------	--

Rationale:

The Event Horizon Telescope (EHT) successfully took a picture of M87's black hole (BH) shadow surrounded by a ringlike emission, which is one of the strongest confirmations of Einstein's general relativity and existence of supermassive BHs at the centers of galaxies. The picture also accelerates our investigations on the launching mechanism of relativistic jets in active galactic nuclei. A puzzling/surprising fact is that M87's jet is unseen in the EHT picture, although it is overwhelmingly bright at longer wavelengths. The missing link between the BH shadow and the jet now draws much attention as one of the most important remaining issues. To address this issue, along with EHT, complementary VLBI observations at long wavelengths (3mm/7mm/10mm), offered by such as the Global Millimeter VLBI Array (GMVA), the Very Long Baseline Array (VLBA) and the East Asian VLBI Network (EAVN) will play increasingly important roles.

The main purpose of this workshop is to get better understanding on BH-powered outflows in the universe. The M87 jet is a prototype in such sources and the first M87 EHT results provide us with a lot of new perspectives on it. Hence, the lineup of invited speakers in this workshop are mostly linked to the first EHT M87 results, and the following topics will be covered by those talks.

Invited Speakers:

- **K. Akiyama** (MIT/NRAO): Next generation EHT & space-VLBI
- **M. Honma** (NAOJ/Mizusawa): Overview of the first EHT results
- **T. Jung** (KASI): KVN/e-KVN
- **T. Kawashima** (NAOJ): BH shadow & jet connection
- **Y. Kawazura** (Tohoku U): Plasma physics in accretion flows
- **J.-Y. Kim** (MPIfR): mmVLBI view of 3C279
- **S. Kisaka** (Tohoku U): BH magnetospheres
- **R. Lu** (SHAO): M87 jet base seen at 3.5mm
- **D. Mazin** (ICRR): High-energy & multi-wavelength science
- **Y. Mizuno** (Goethe U Frankfurt): BH shadow & gravity theories
- **M. Nakamura** (ASIAA): Jet theories & simulations
- **K. Niinuma** (Yamaguchi U): EAVN-high
- **K. Ohsuga** (U Tsukuba): BH high-power accretion & outflow
- **J. Park** (ASIAA): M87 jet velocity & surrounding wind



EHT観測結果の理論的解釈と将来展望

~高エネルギー宇宙物理の視点~





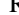



















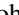
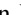



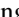
















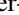
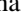

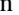

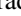




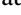



当真賢二 (Kenji TOMA)

FRIS, Tohoku University

The Event Horizon Telescope Collaboration

Kazunori Akiyama^{1,2,3,4} , Antxon Alberdi⁵ , Walter Alef⁶ , Keiichi Asada⁷ , Rebecca Azulay^{8,9,6} , Anne-Kathrin Baczko⁶ , David Ball¹⁰ , Mislav Baloković^{4,11} , John Barrett² , Dan Bintley¹² , Lindy Blackburn^{4,11} , Wilfred Boland¹³ , Katherine L. Bouman^{4,11,14} , Geoffrey C. Bower¹⁵ , Michael Bremer¹⁶ , Christiaan D. Brinkerink¹⁷ , Roger Brissenden^{4,11} , Silke Britzen⁶ , Avery E. Broderick^{18,19,20} , Dominique Brogiere¹⁶ , Thomas Bronzwaer¹⁷ , Do-Young Byun^{21,22} , John E. Carlstrom^{23,24,25,26} , Andrew Chael^{4,11} , Chi-kwan Chan^{10,27} , Shami Chatterjee²⁸ , Koushik Chatterjee²⁹ , Ming-Tang Chen¹⁵ , Yongjun Chen (陈永军)^{30,31} , Ilje Cho^{21,22} , Pierre Christian^{10,11} , John E. Conway³² , James M. Cordes²⁸ , Geoffrey B. Crew² , Yuzhu Cui^{33,34} , Jordy Davelaar¹⁷ , Mariafelicia De Laurentis^{35,36,37} , Roger Deane^{38,39} , Jessica Dempsey¹² , Gregory Desvignes⁶ , Jason Dexter⁴⁰ , Sheperd S. Doeleman^{4,11} , Ralph P. Eatough⁶ , Heino Falcke¹⁷ , Vincent L. Fish² , Ed Fomalont¹ , Raquel Fraga-Encinas¹⁷ , Per Friberg¹² , Christian M. Fromm³⁶ , José L. Gómez⁵ , Peter Galison^{1,41,42} , Charles F. Gammie^{43,44} , Roberto García¹⁶ , Olivier Gentaz¹⁶ , Boris Georgiev^{19,20} , Ciriaco Goddi^{17,45} , Roman Gold³⁶ , Minfeng Gu (顾敏峰)^{30,46} , Mark Gurwell¹¹ , Kazuhiro Hada^{33,34} , Michael H. Hecht² , Ronald Hesper⁴⁷ , Luis C. Ho (何子山)^{48,49} , Paul Ho⁷ , Mareki Honma^{33,34} , Chih-Wei L. Huang⁷ , Lei Huang (黄磊)^{30,46} , David H. Hughes⁵⁰ , Shiro Ikeda^{3,51,52,53} , Makoto Inoue⁷ , Sara Issaoun¹⁷ , David J. James^{4,11} , Buell T. Jannuzi¹⁰ 



Bart Kipperda¹⁰ , Freek Roelofs¹⁰ , Alan Rogers¹⁰ , Eduardo Ros¹⁰ , Meri Rose¹⁰ , Arash Roshanmehsari¹⁰ , Heide Rothmann¹⁰ , Alan L. Roy⁶ , Chet Ruszczyk² , Benjamin R. Ryan^{80,81} , Kazi L. J. Rygl⁶³ , Salvador Sánchez⁸² , David Sánchez-Argüelles^{50,83} , Mahito Sasada^{33,84} , Tuomas Savolainen^{6,85,86} , F. Peter Schloerb⁷⁴ , Karl-Friedrich Schuster¹⁶ , Lijing Shao^{6,49} , Zhiqiang Shen (沈志强)^{30,31} , Des Small⁵⁶ , Bong Won Sohn^{21,22,87} , Jason SooHoo² , Fumie Tazaki³³ , Paul Tiede^{19,20} , Remo P. J. Tilanus^{17,45,88} , Michael Titus² , Kenji Toma^{89,90} , Pablo Torne^{6,82} , Tyler Trent¹⁰ , Sascha Trippe⁹¹ , Shuichiro Tsuda³³ , Ilse van Bemmelen⁵⁶ , Huib Jan van Langevelde^{56,92} , Daniel R. van Rossum¹⁷ , Jan Wagner⁶ , John Wardle⁹³ , Jonathan Weintraub^{4,11} , Norbert Wex⁶ , Robert Wharton⁶ , Maciek Wielgus^{4,11} , George N. Wong⁴³ , Qingwen Wu (吴庆文)⁹⁴ , André Young¹⁷ , Ken Young¹¹ , Ziri Younsi^{95,36} , Feng Yuan (袁峰)^{30,46,96} , Ye-Fei Yuan (袁业飞)⁹⁷ , J. Anton Zensus⁶ , Guangyao Zhao²¹ , Shan-Shan Zhao^{17,61} , Ziyang Zhu⁴² , Jacyk Anczarski⁹⁸ , Frederick K. Baganoff⁹⁹ , Andreas Eckart^{6,100} , Joseph R. Farah^{11,101,4} , Daryl Haggard^{102,103,104} , Zheng Meyer-Zhao^{7,105} , Daniel Michalik^{106,107} , Andrew Nadolski⁴⁴ , Joseph Neilsen⁹⁸ , Hiroaki Nishioka⁷ , Michael A. Nowak¹⁰⁸ , Nicolas Pradel⁷ , Rurik A. Primiani¹⁰⁹ , Kamal Souccar⁷⁴ , Laura Vertatschitsch^{11,109} , Paul Yamaguchi¹¹ , and Shuo Zhang⁹⁹ 

Event Horizon Telescope

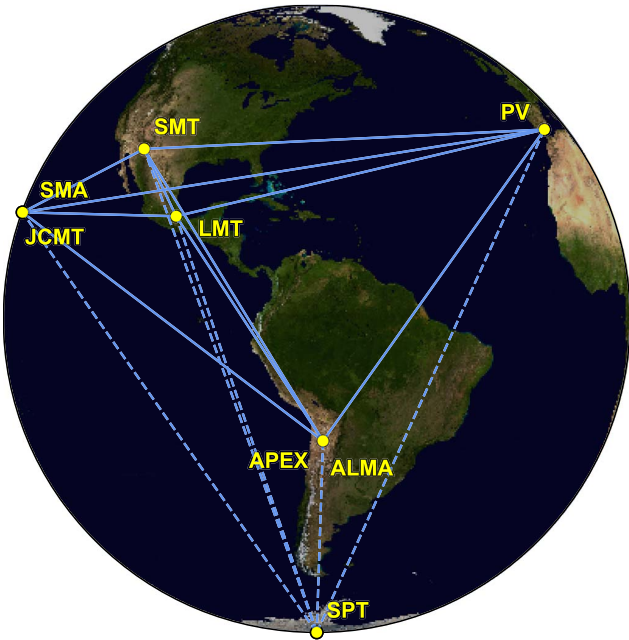


Figure 1. Eight stations of the EHT 2017 campaign over six geographic locations as viewed from the equatorial plane. Solid baselines represent mutual visibility on M87* (+12° declination). The dashed baselines were used for the calibration source 3C279 (see Papers [III](#) and [IV](#)).

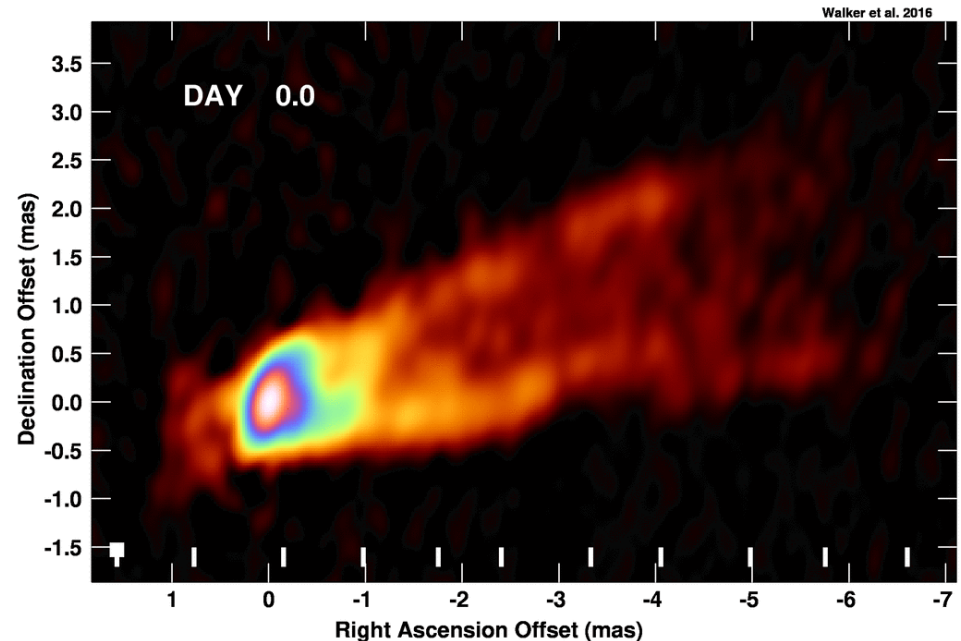
<i>Object</i>	M_{BH} ($10^8 M_{sun}$)	d (Mpc)	$1Rs$ (μas)
<i>SgrA*</i>	0.04	0.008	10
<i>M87</i>	60	16.7	7
<i>Sombrero</i>	10	9.0	2.2
<i>M84</i>	8.5	17	1
<i>Cen A</i>	0.5	3.8	0.3

Photon ringの直径は $\sim 5 R_s$

- Technical developments for VLBI at 1.3 mm (230 GHz)
- Angular resolution $\theta \sim 1.3 \text{ mm}/10^4 \text{ km} \sim 25 \mu as$

M87

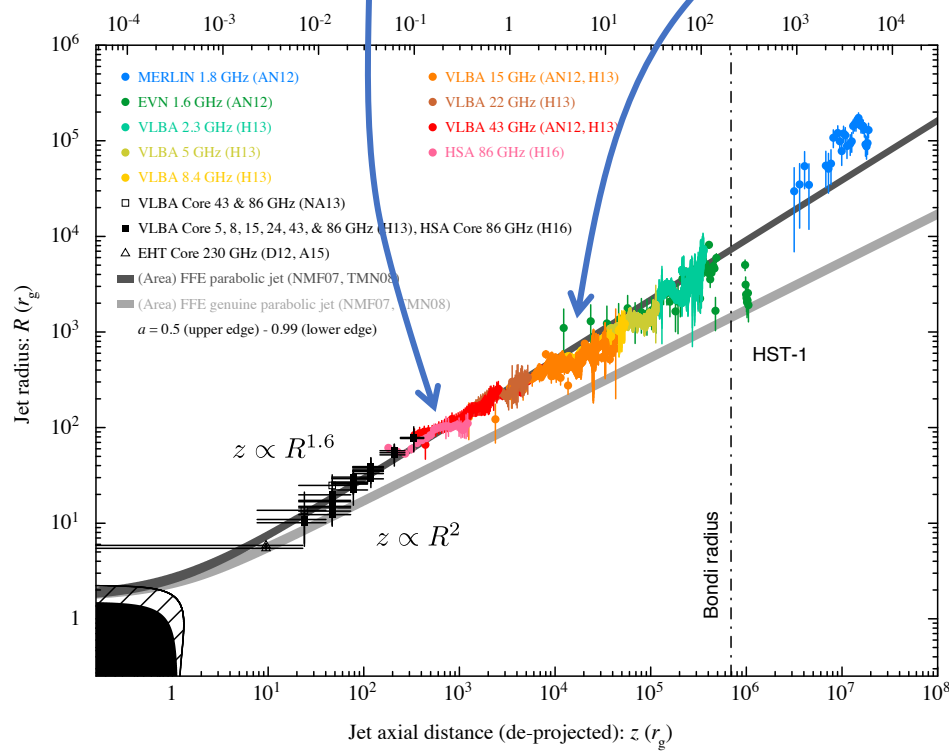
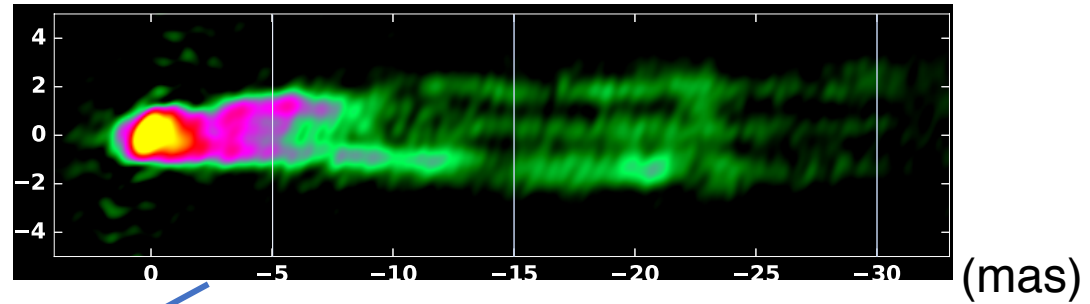
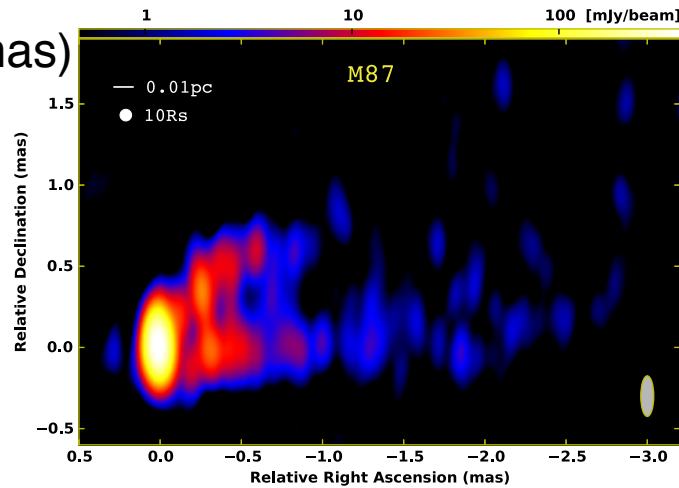
- Low-luminosity AGN with $L_\gamma \sim 10^{42} \text{ erg/s} \sim 10^{-6} L_{\text{Edd}}$ (for $M_{\text{BH}} \sim 6 \times 10^9 M_{\text{sun}}$)
 - Radiatively inefficient accretion flow (RIAF)
 - $r_g \sim 10^{15} \text{ cm}$, $r_g/c \sim 10 \text{ hr}$
- Radio jet (FR I type)
 - $L_{\text{jet}} \sim 10^{42} - 10^{45} \text{ erg/s}$
 - BZ process?
 - $L_{\text{jet}} \sim \dot{M} c^2$?



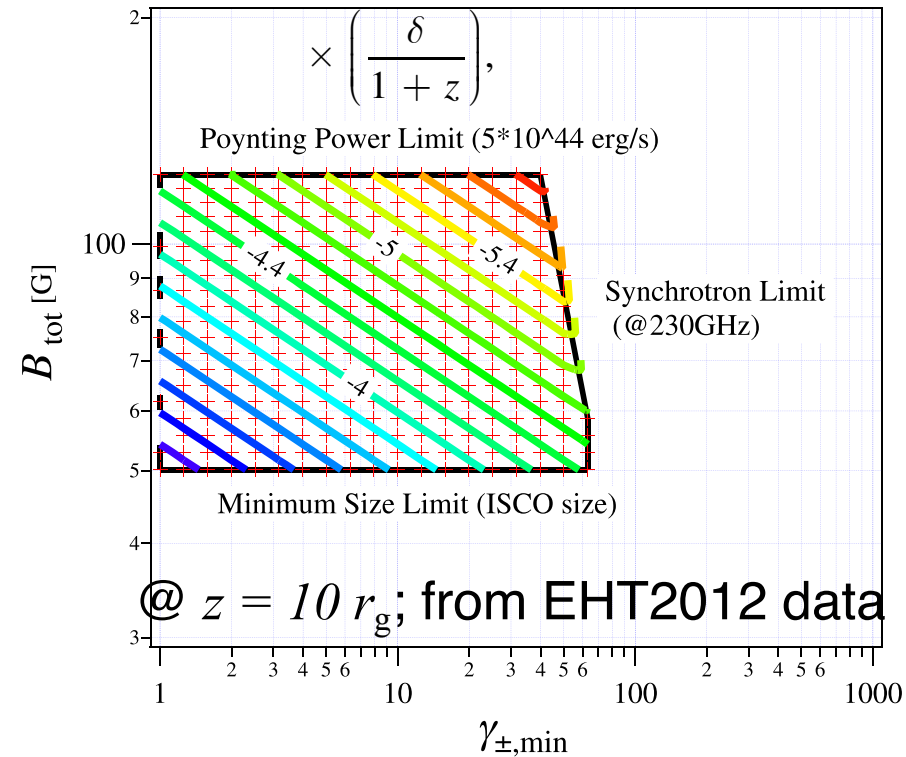
86 GHz (3.5mm); VLBA+GBT

15 GHz; VLBA+VLA (*VSOP* also detected the triple-ridge)

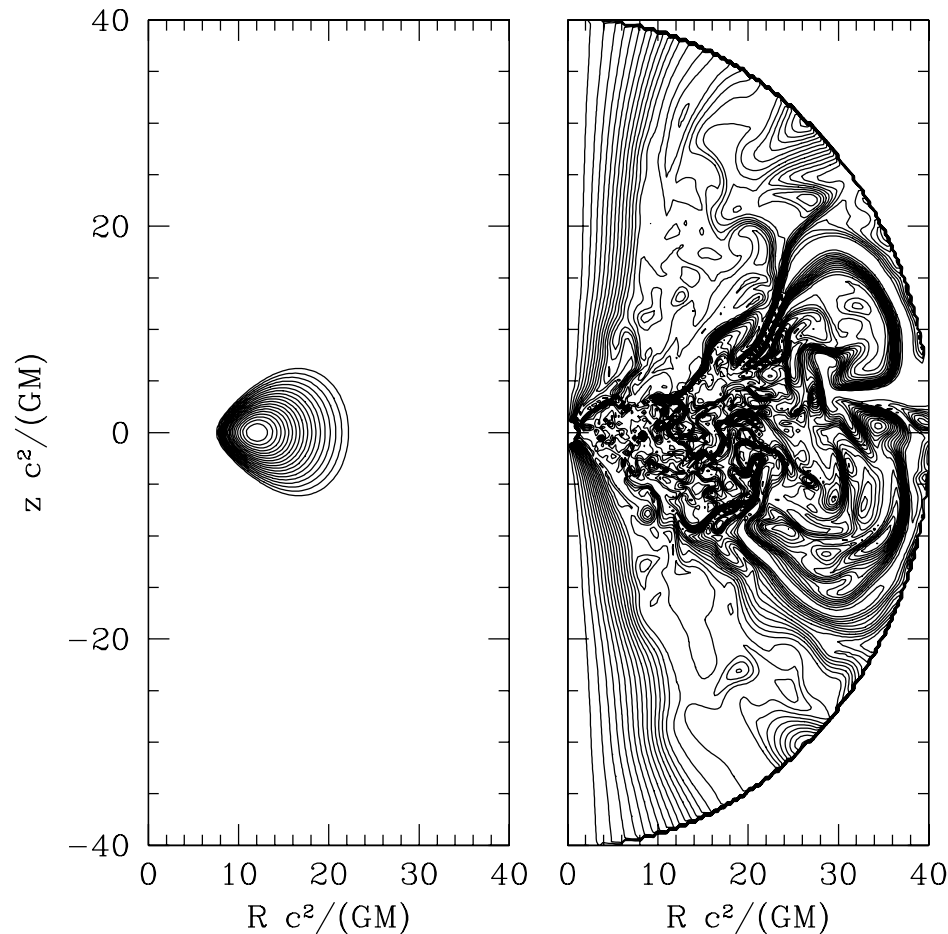
(mas)



$$B_{\perp} = b(p) \left(\frac{\nu_{\text{ssa,obs}}}{1 \text{ GHz}} \right)^5 \left(\frac{\theta_{\text{obs}}}{1 \text{ mas}} \right)^4 \left(\frac{S_{\nu_{\text{ssa,obs}}}}{1 \text{ Jy}} \right)^{-2}$$



GRMHD simulations



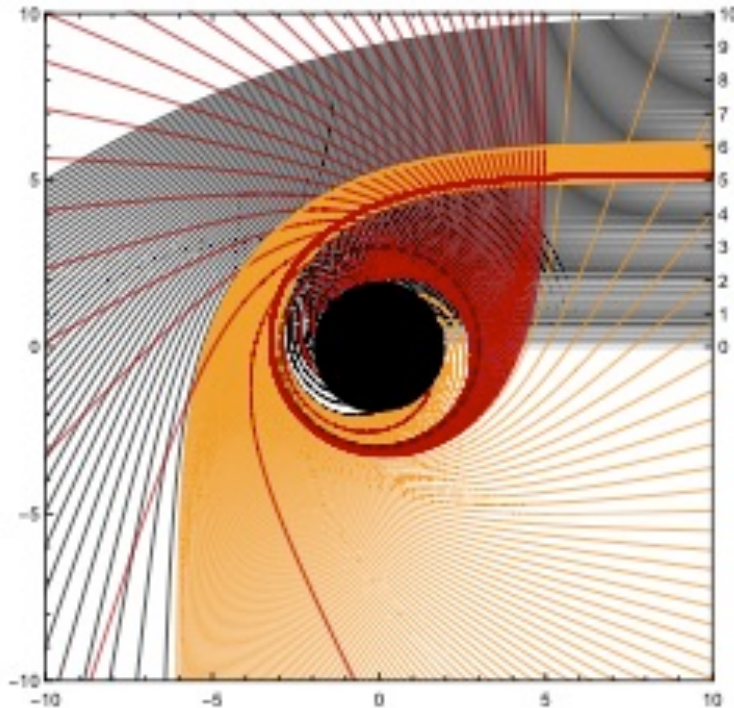
- Magnetohydrodynamic simulations in fixed Kerr spacetime
- Radiatively inefficient accretion flow (RIAF)
- Spinning BH-driven jet where $B^2/\rho c^2 \gg 1$ via Blandford-Znajek process

Blandford & Znajek 1977;
KT & Takahara 2014;2016

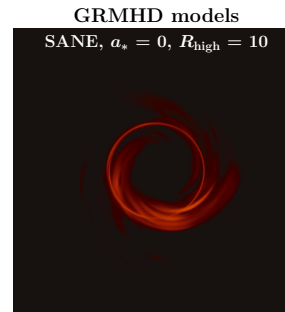
e.g. Koide et al. 2000; Komissarov 2001;
McKinney & Gammie 2004; Noble+2006
Barkov & Komissarov 2008; Tchekhovskoy et al.
2011; Ruiz et al. 2012; Contopoulos et al. 2013

Black hole shadow & photon ring

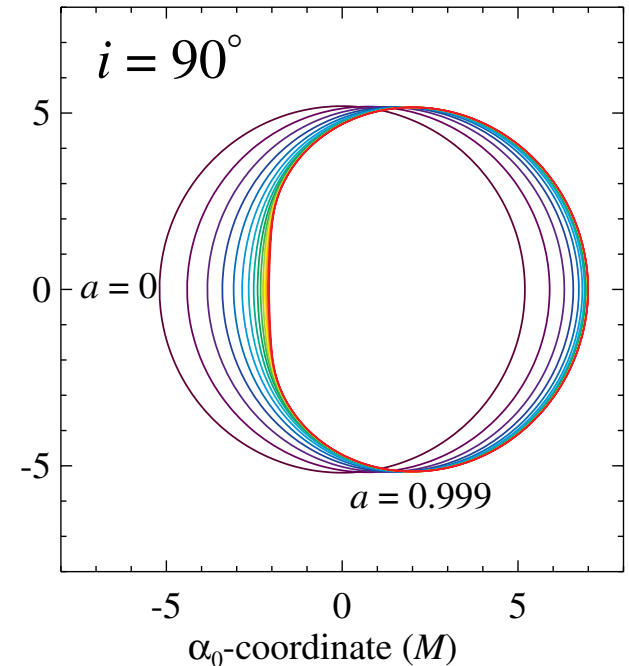
Zero-spin BH with emitting plane



$\updownarrow 3\sqrt{3} r_g$



Simulated EHT observations



- Photons will have orbited the BH many times (near the unstable orbit), picking up extra brightness on their way to the observer

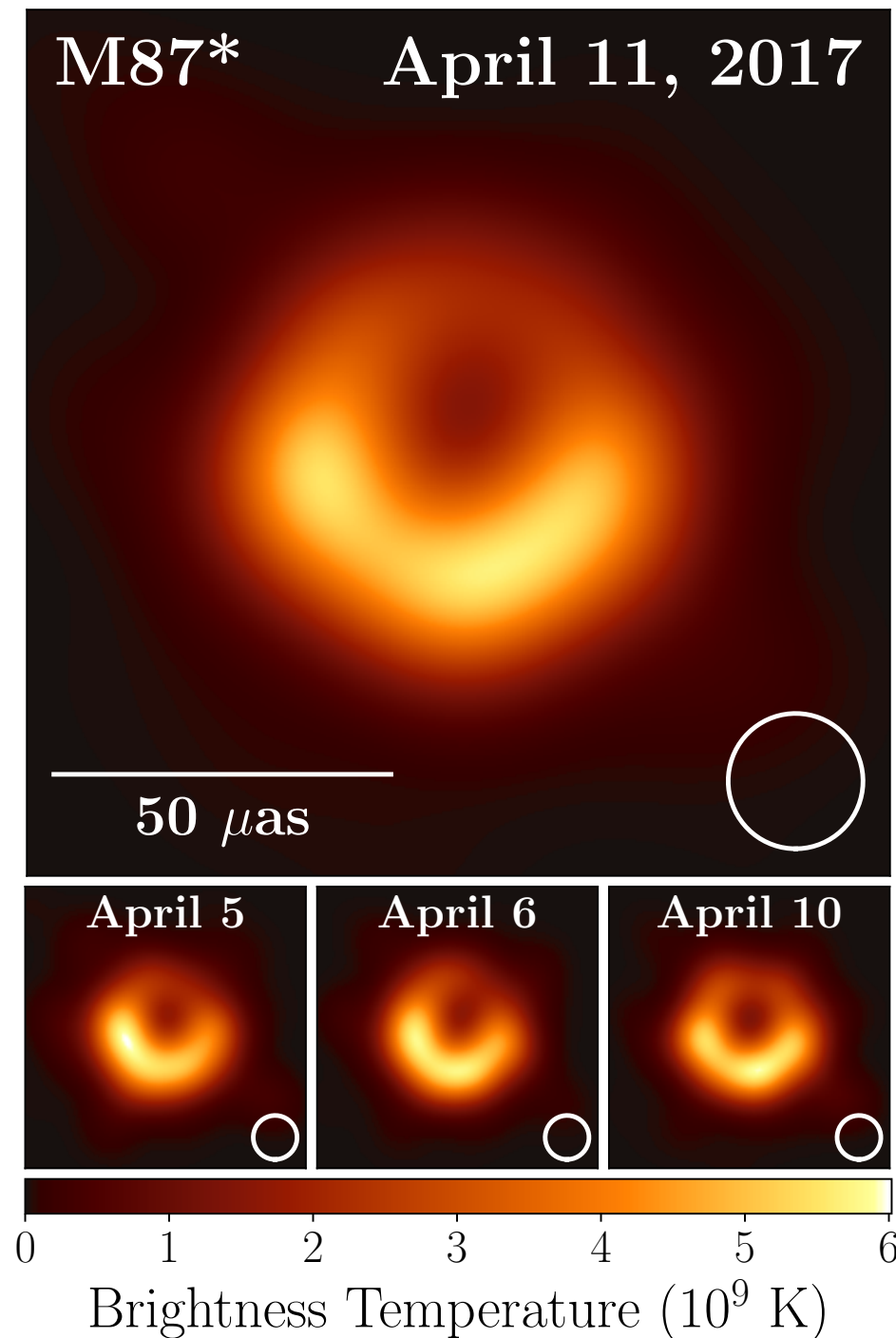
- The shadow shape does NOT strongly depend on BH spin

EHT images

- Central depression in brightness with a flux ratio $>\sim 10:1$
- Ring shape
 - no extended component (jet / accretion disk)
→ EHT 2020
- Flux ~ 0.5 Jy
- Asymmetry
- Stable in different days

$$F_\nu \simeq 0.5 \text{ Jy}$$

$$\times \left(\frac{\theta}{40 \mu\text{as}} \right)^2 \left(\frac{\nu}{230 \text{ GHz}} \right)^2 \frac{T_b}{6 \times 10^9 \text{ K}}$$



Paper V: Physical origin of the asymmetric ring

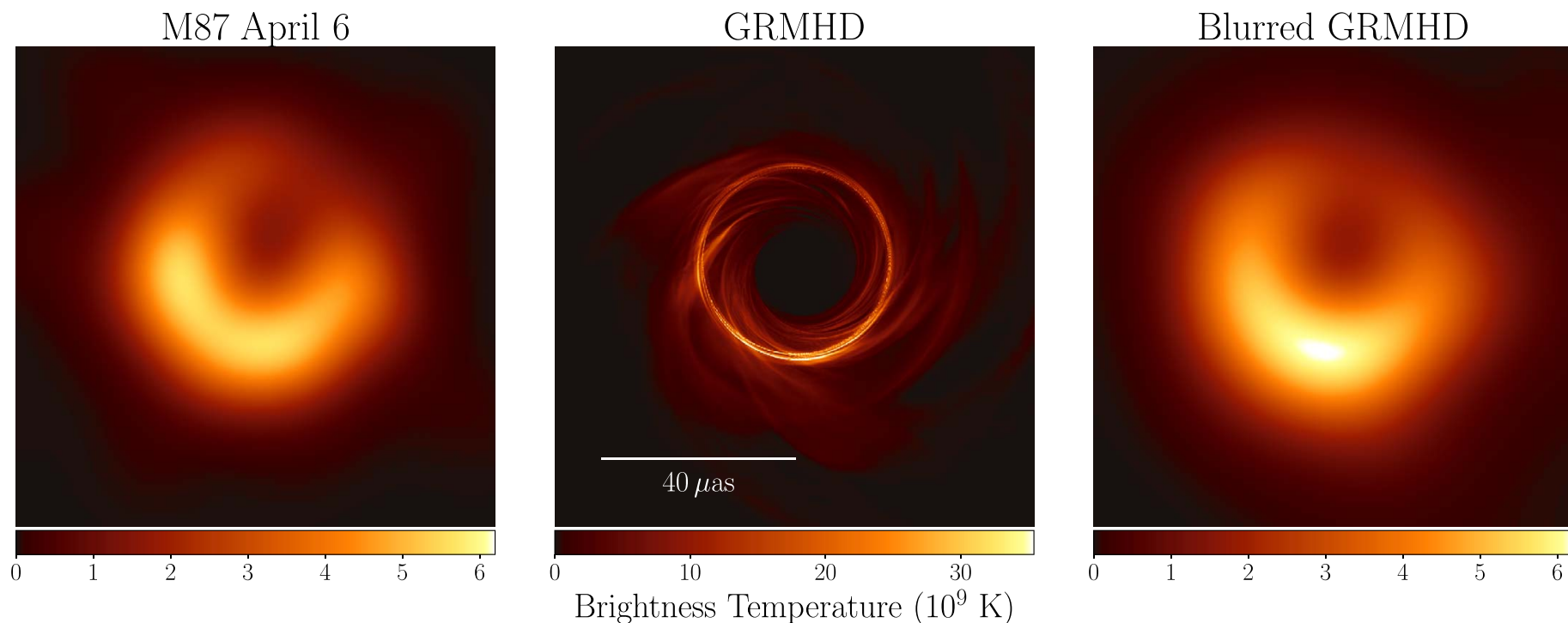


Figure 1. Left panel: an EHT2017 image of M87 from Paper IV of this series (see their Figure 15). Middle panel: a simulated image based on a GRMHD model. Right panel: the model image convolved with a $20 \mu\text{as}$ FWHM Gaussian beam. Although the most evident features of the model and data are similar, fine features in the model are not resolved by EHT.

- Working hypothesis: Kerr BH with $-1 < a_* = Jc/GM^2 < 1$
 - GRMHD simulations + GRRT imaging
- Examine if the model is consistent with the EHT data

Rough estimates

$$T_i \sim 0.3 T_{i,\text{vir}} \simeq 10^{12} \left(\frac{r_g}{r} \right) \text{ K}$$

$$\left\{ \begin{array}{l} n_i k_B T_i + n_e k_B T_e = \beta_p B^2 / 8\pi \\ F_\nu = \frac{4\pi r^3 n_e}{3D^2} \left[\sqrt{2}\pi \frac{e^2 \nu_s}{6\pi \Theta_e^2 c} \left(\frac{\nu}{\nu_s} \right) e^{-\left(\frac{\nu}{\nu_s} \right)^{\frac{1}{3}}} \right] \\ \sim 0.5 \text{ Jy} \end{array} \right. \quad \begin{array}{l} \text{Optically-thin} \\ \text{thermal } e \text{ synchrotron} \\ \text{(Leung+2011)} \end{array}$$

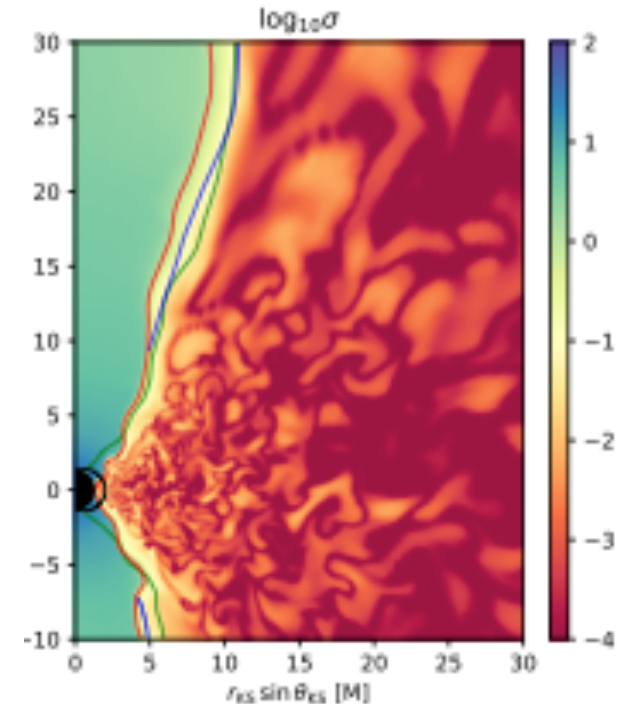
$$\nu_s = \frac{eB}{9\pi m_e c} \Theta_e^2 \sim 0.3 \left(\frac{\Theta_e}{10} \right)^2 \text{ GHz} \ll 230 \text{ GHz} \quad F_\nu \propto r^3 n_e B^3 T_e^4$$

$$n_e \simeq 3 \times 10^4 \left(\frac{r}{r_g} \right)^{-1.3} \beta_p^{0.62} \left(\frac{T_i}{3T_e} \right)^{-0.47} \left(\frac{T_e}{10T_b} \right)^{-2.4} \text{ cm}^{-3}$$

$$B \simeq 5 \left(\frac{r}{r_g} \right)^{-0.63} \beta_p^{-0.19} \left(\frac{T_i}{3T_e} \right)^{0.14} \left(\frac{T_e}{10T_b} \right)^{-0.71} \text{ G} \quad T_b \sim 6 \times 10^9 \text{ K}$$

GRMHD simulation library

- Kerr BH with fixed M & a_*
- 3D ideal MHD models
- Codes: BHAC (Porth+17), H-AMR (Liska+18), iharm (Gammie+03), KORAL (Sadowski+13)
- Initial condition: hydrodynamically static torus + poloidal B field
 - Accretion flow AM || BH spin
- Outflow-only boundary condition
- Density floor



Porth+ 2019

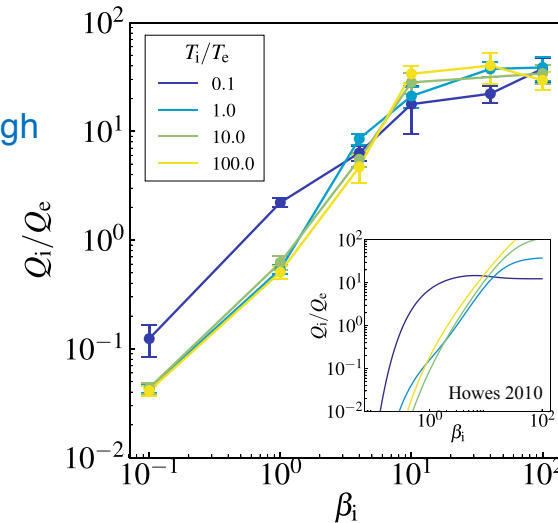
- Quasi-steady state at $r < \sim 10 r_g$: $5000 < \sim t/r_g c^{-1} < \sim 10^4$
- 2 key parameters: normalized magnetic flux & BH spin
 - SANE models ($\phi \sim 3$): $a_* = -0.94, -0.5, 0, 0.5, 0.75, 0.88, 0.94, 0.97, 0.98$
 - MAD models ($\phi > 50$): $a_* = -0.94, -0.5, 0, 0.5, 0.75, 0.94$

$$\phi \equiv \Phi_{\text{BH}} (\dot{M} r_g^2 c)^{-1/2}$$

GR Ray-Tracing calculations

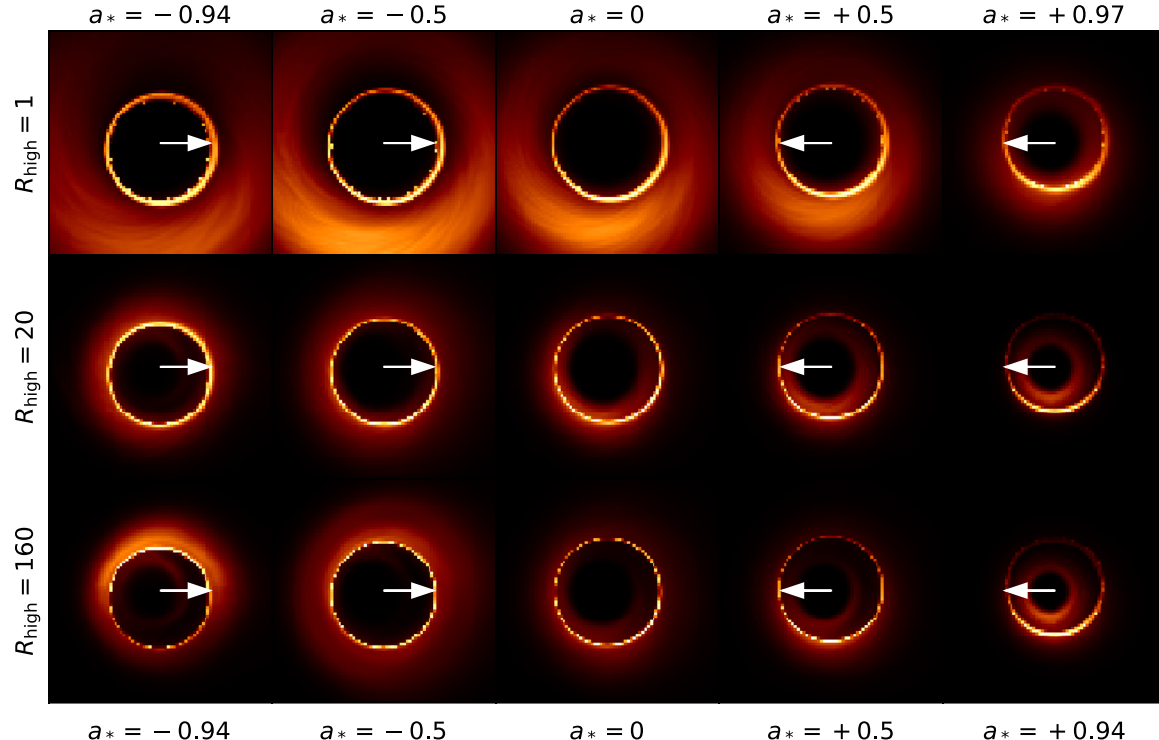
- Thermal electrons assumed, with one parameter R_{high} (cf. Howes 2006; Kawazura+2018)

$$R \equiv \frac{T_i}{T_e} = R_{\text{high}} \frac{\beta_p^2}{1 + \beta_p^2} + \frac{1}{1 + \beta_p^2}$$

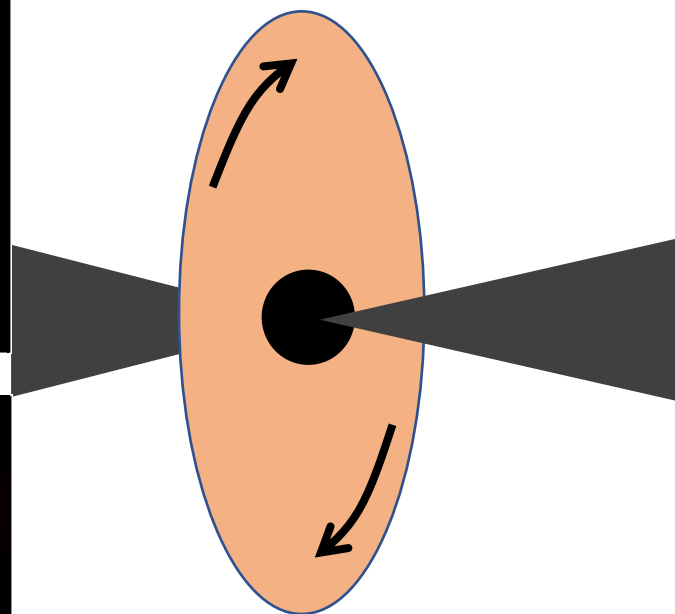


- Emission from regions with $B^2 > \rho c^2$ (i.e. funnel region) is set to zero
- 100-500 images from each GRMHD models, each of $R_{\text{high}} = 1, 10, 20, 40, 80, 160$
inclination $i = 12^\circ, 17^\circ, 22^\circ, 158^\circ, 163^\circ, 168^\circ$ (not highly affect image)
- Various codes that include RAIKOU (Kawashima+)
- MHD velocity field is invariant under scaling $\rho \rightarrow C\rho, B \rightarrow C^{1/2}B, u \rightarrow Cu$
- C is adjusted for $F_v \sim 0.5$ Jy, then M determines ring size & $\dot{M} \sim 4\pi r^2 \rho v^r$

SANE

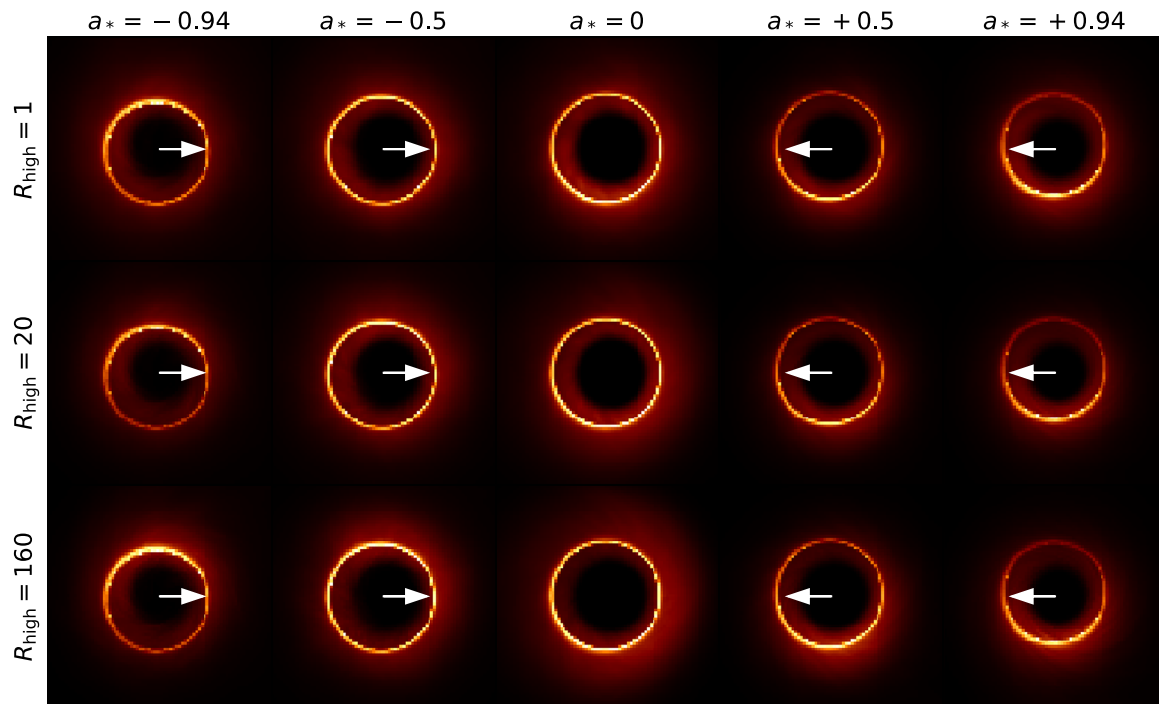


- Time-averaged images
- $i = 163$ deg (Accretion disk angular momentum)
- Arrows: BH spin vector projected onto the sky

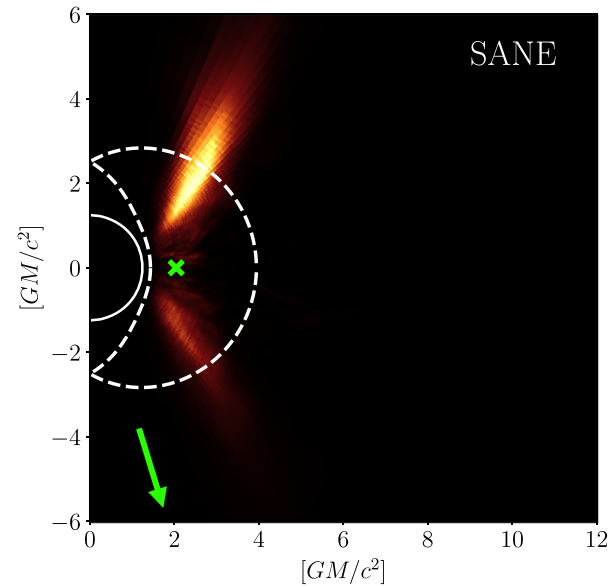
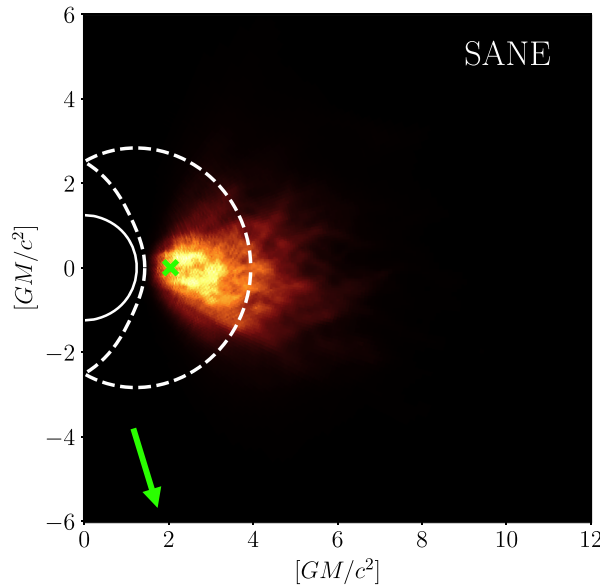
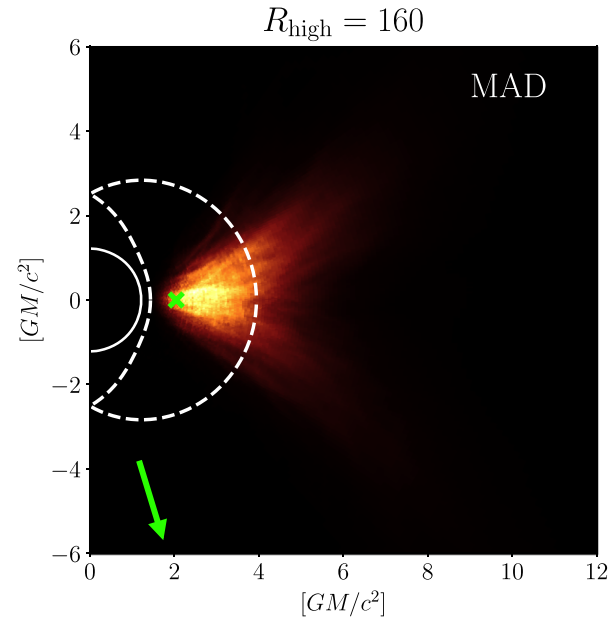
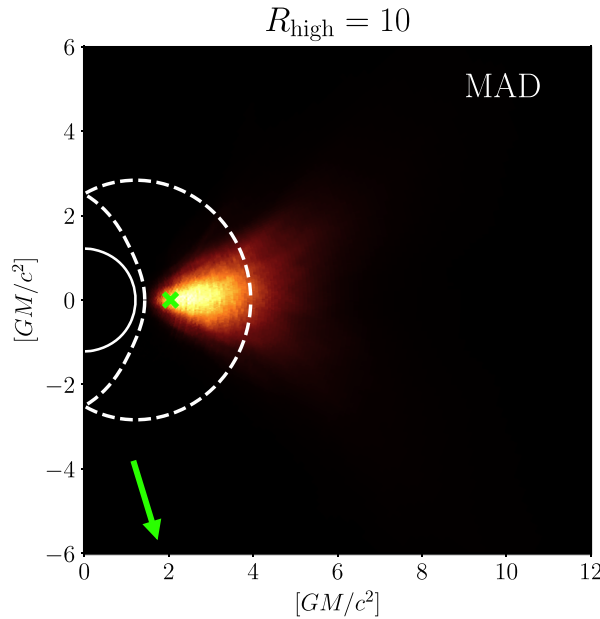


- So many models are acceptable. This is likely because the source structure is dominated by the photon ring
- Asymmetry is controlled by the BH spin (except the SANE $R_{\text{high}} < 10$)

MAD



- Prograde models: $a_* > 0$
- Location of the origin for all photons that make up an image
- Emission at $1 < r/r_g < 4$ (unstable photon orbit region) dominant
- The funnel wall is bright for high R_{high} cases
- Funnel is wider for MAD than for SANE



Other constraints

- Radiative efficiency
 - $L_{\text{bol}}/\dot{M} c^2 < \text{thin disk radiative efficiency}$
- Simultaneous X-ray observation (2-10 keV)
 - Single IC scattering of synchrotron photons
- $P_{\text{jet}} \sim 10^{42} - 10^{45} \text{ erg/s}$
 - Conservative lower limit: 10^{42} erg/s
 - All $a_*=0$ models rejected
 - SANE models with $|a_*|=0.5$ rejected

$$P_{\text{BZ}} \approx 2.8 f(a_*) (\phi/50)^2 \dot{M} c^2 \quad f(a_*) \approx a_*^2 (1 + \sqrt{1 - a_*^2})^{-2} \\ \text{(for } a_* < 0.95\text{)}$$

Other constraints

- EHT image, radiative efficiency, X-ray, jet power

a/R_{high}	1	10	20	40	80	160
-0.94	----	++++	++++	++++	++++	----
-0.5	++--	++--	++++	++++	----	++--
0	++++	++++	++--	++++	++--	++--
0.5	++++	++++	++++	++++	++++	++++
0.94	++--	++--	++++	++++	++++	++++

SANE

$$\dot{M}/\dot{M}_{\text{Edd}} \sim 10^{-5} - 10^{-4}$$

$$\dot{M}_{\text{Edd}} = 10 L_{\text{Edd}}/c^2$$

a/R_{high}	1	10	20	40	80	160
-0.94	--++	++++	++++	++++	++++	++++
-0.5	++--	++++	++++	++++	++++	++++
0	++--	++++	++++	++++	++++	++++
0.5	++--	++++	++++	++++	++++	++++
0.94	+- -+	++++	++++	++++	++++	++++

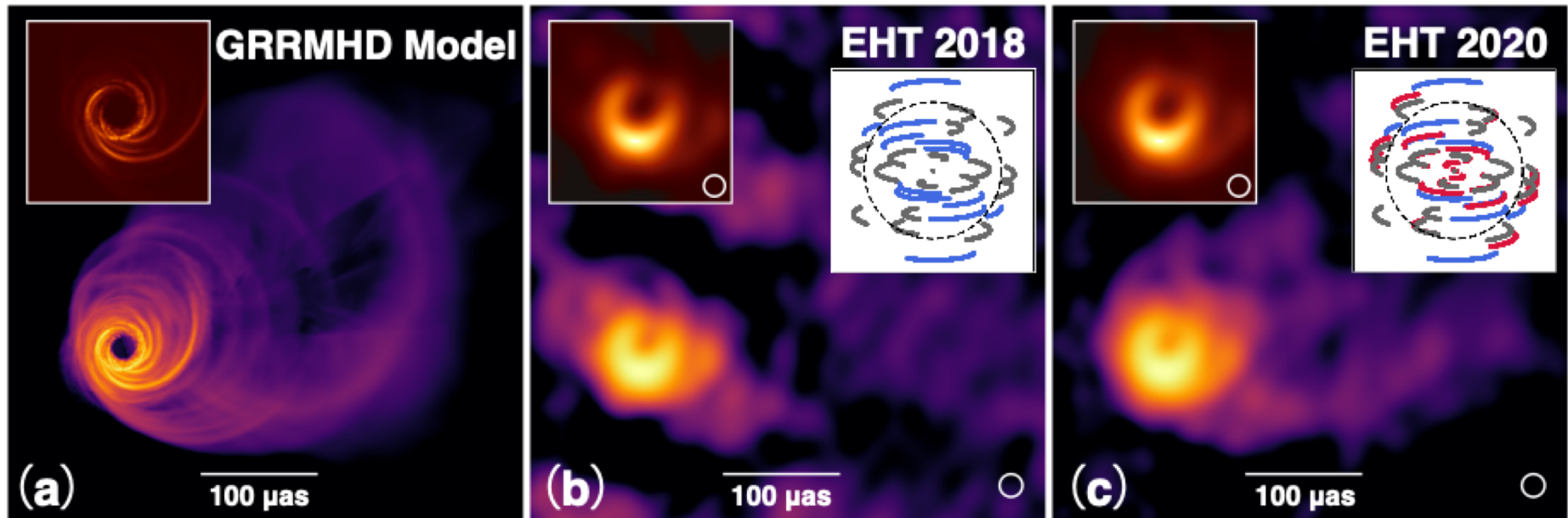
MAD

$$\dot{M}/\dot{M}_{\text{Edd}} \sim 10^{-6}$$

EHT2017 Summary

- EHT 2017 data are consistent with the hypothesis that
 - 1.3 mm emission arises within a few r_g of a Kerr BH
 - Optically-thin synchrotron emission of thermal electron in RIAF
 - Image is generated by strong grav. lensing & Doppler beaming
- $M = 6.5^{+0.7}_{-0.6} \times 10^9 M_{\text{sun}}$ ($M/D = 3.8^{+0.4}_{-0.3} \mu\text{as}$), which is consistent with previous estimate based on stellar dynamics
- The strongest evidence for the presence of SMBHs in centers of galaxies
- Case of $a_* = 0$ rejected by condition $P_{\text{jet}} > 10^{42} \text{ erg/s}$
- The jet is driven via BZ process in the models with $a_* \neq 0$

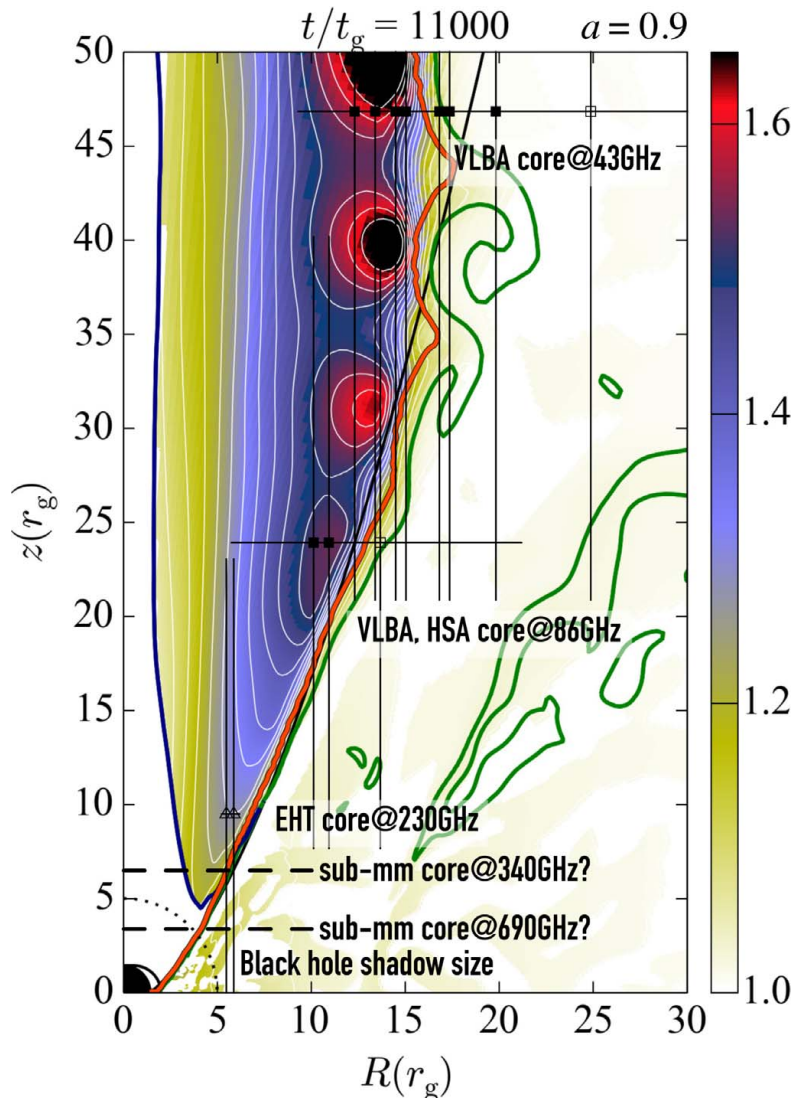
EHT 2020 forecast



- EHT Collaboration, ALMA Cycle 7 M87 Proposal
- 3 more telescopes including Green Land Telescope will make it so sensitive as to detect extended component

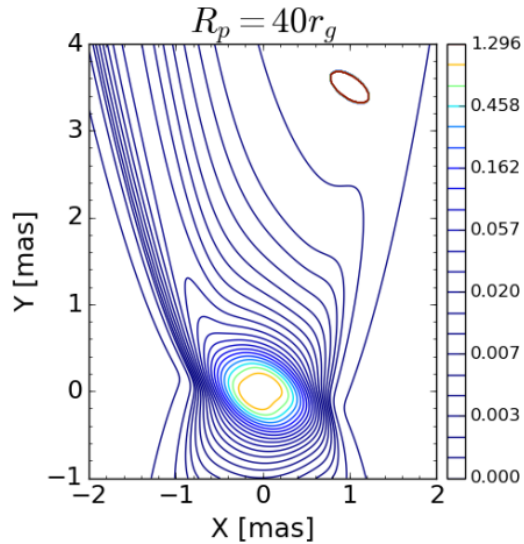
Connection of the ring with the jet

Nakamura+2018

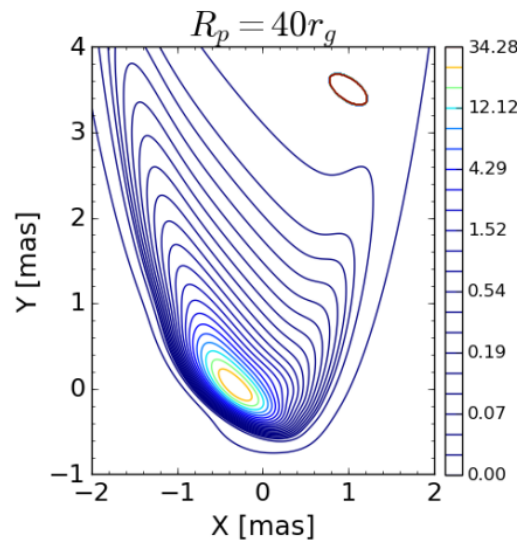


- 2D high-resolution MHD simulation
 - Stagnation surface
 - Relativistic blobs by MHD instability?
- What is an observational evidence of the BZ process for the jet production?
- Observed relativistic blobs --- $\sigma > \text{a few}$
- B strength estimates from core size (Kino)
- Sharp limb-brightening (K. Takahashi)
- Only jet edge shines?
 - No effective particle injection (Shigeo)
 - Gap formation – null surface (Kisaka)
 $n_{GJ} \sim B/(4\pi e r_g) \sim 10^{-5} B_2/M_9 \text{ cm}^{-3}$
 - Gamma-ray origin?
- Spine emission? (Ogihara; Shuta)

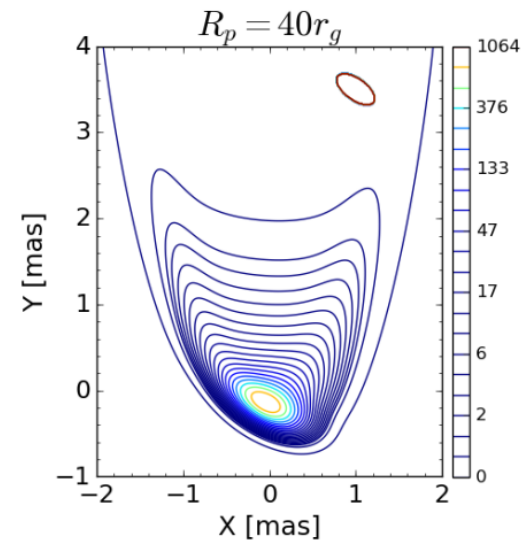
Keplerian disk



Kerr BH with $a=0.1$



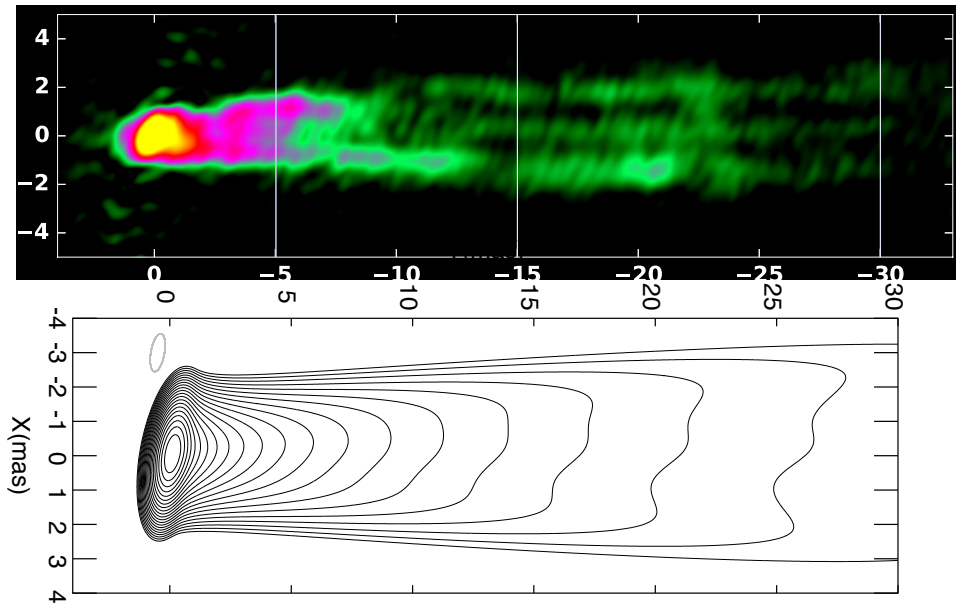
Kerr BH with $a=0.998$



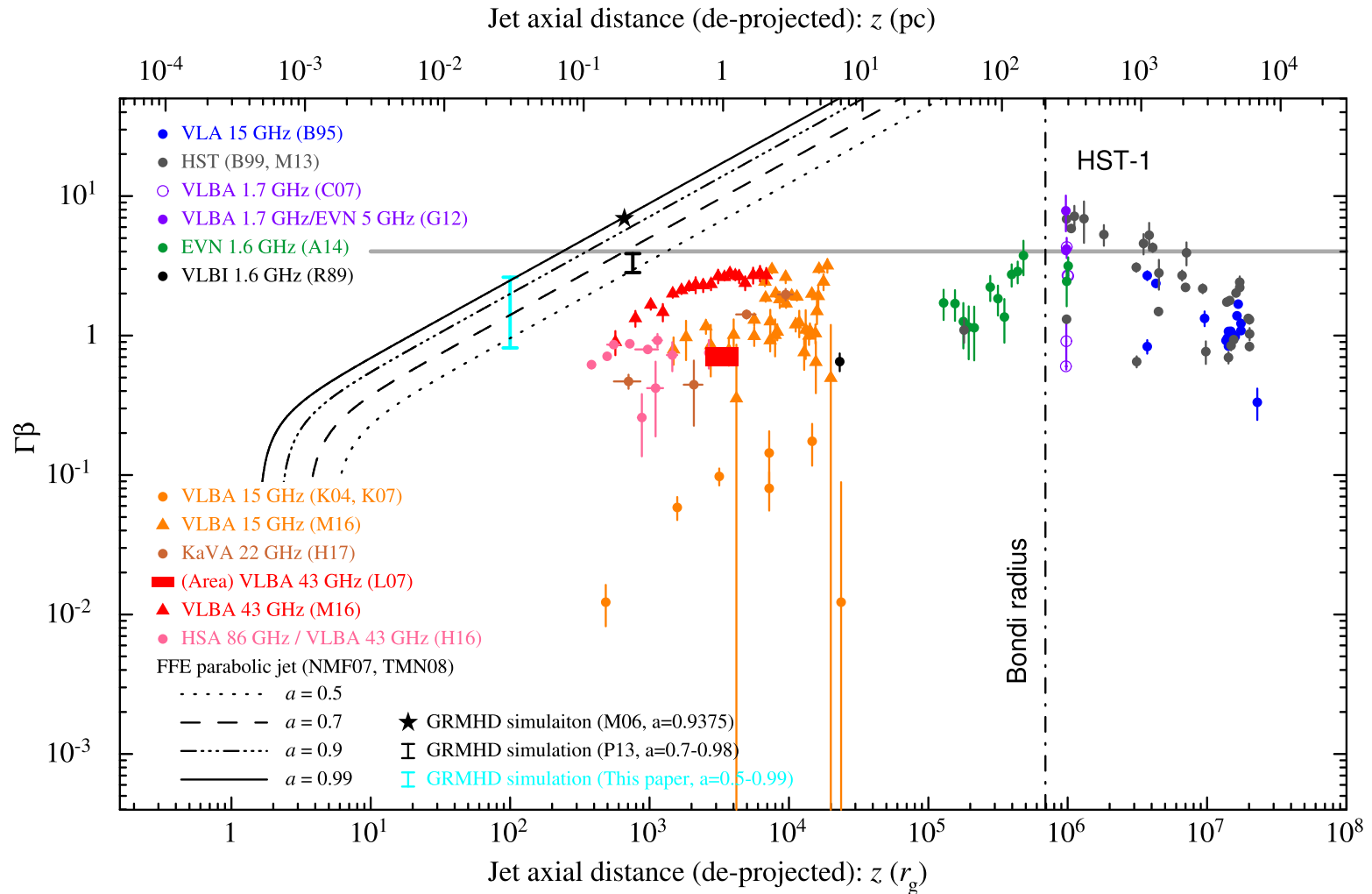
$$\Psi = Ar^\nu(1 \mp \cos \theta). \quad B_\phi = \mp \frac{2\Omega_F \Psi}{Rc},$$

$$\mathbf{v} = \frac{\mathbf{E} \times \mathbf{B}}{B^2} c :$$

- Faster rotation, $v_p \gg v_\phi$,
Less asymmetric &
Dimmer counter-jet
- But limb is not so sharp



M87 proper motion



Jet edge: mass mixing reduces velocity?

M87 spectrum

- Jet SSC model
 $r \sim 10^{16}$ cm
 $B \sim 55$ mG
- Matter dominant
 at $10 r_g$?

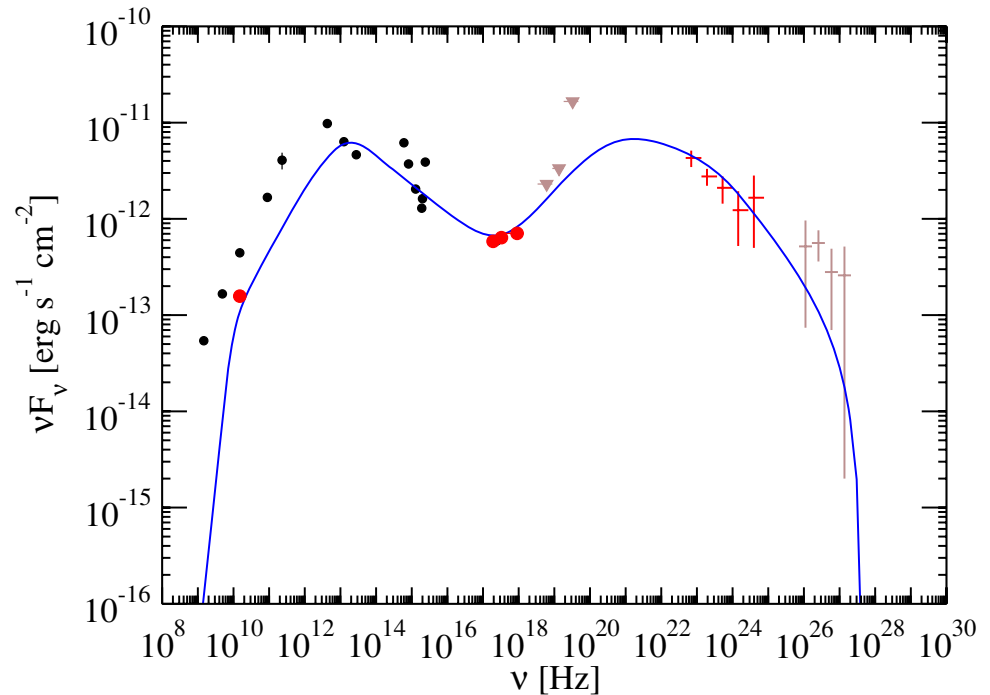
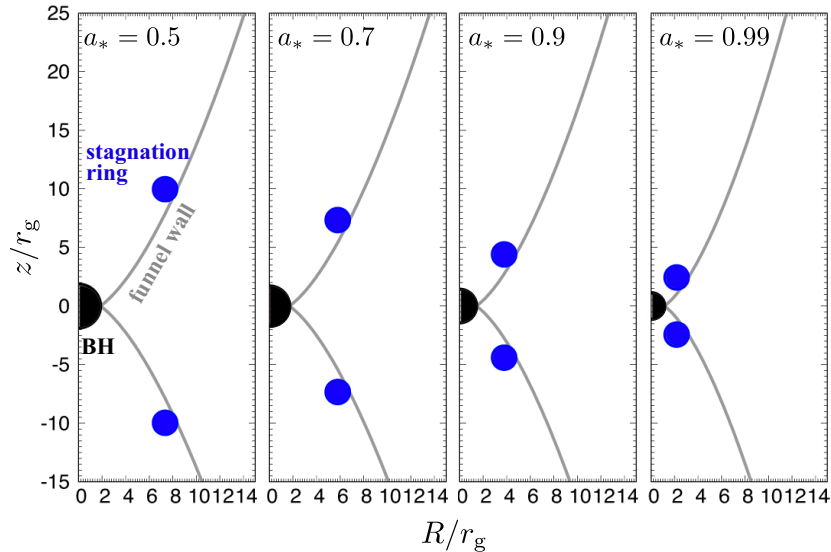


Figure 4. SED of M87 with the LAT spectrum and the 2009 January 7 MOJAVE VLBA 15 GHz and *Chandra* X-ray measurements of the core indicated in red. The non-simultaneous 2004 TeV spectrum described in Figure 2 and *Swift*/BAT hard X-ray limits (Section 3) of the integrated emission are shown in light brown. Historical measurements of the core from VLA 1.5, 5, 15 GHz (Biretta et al. 1991), IRAM 89 GHz (Despringre et al. 1996), SMA 230 GHz (Tan et al. 2008), *Spitzer* 70, 24 μ m (Shi et al. 2007), Gemini 10.8 μ m (Perlman et al. 2001), *Hubble Space Telescope HST* optical/UV (Sparks et al. 1996), and *Chandra* 1 keV from Marshall et al. (2002, hidden behind the new measurements) are plotted as black circles. The VLBA 15 GHz flux is systematically lower than the historical arcsec-resolution radio to infrared measurements due to the presence of intermediate scale emission (see, e.g., Kovalev et al. 2007). The blue line shows the one-zone SSC model fit for the core described in Section 3.

Stagnation ring model (Preliminary)

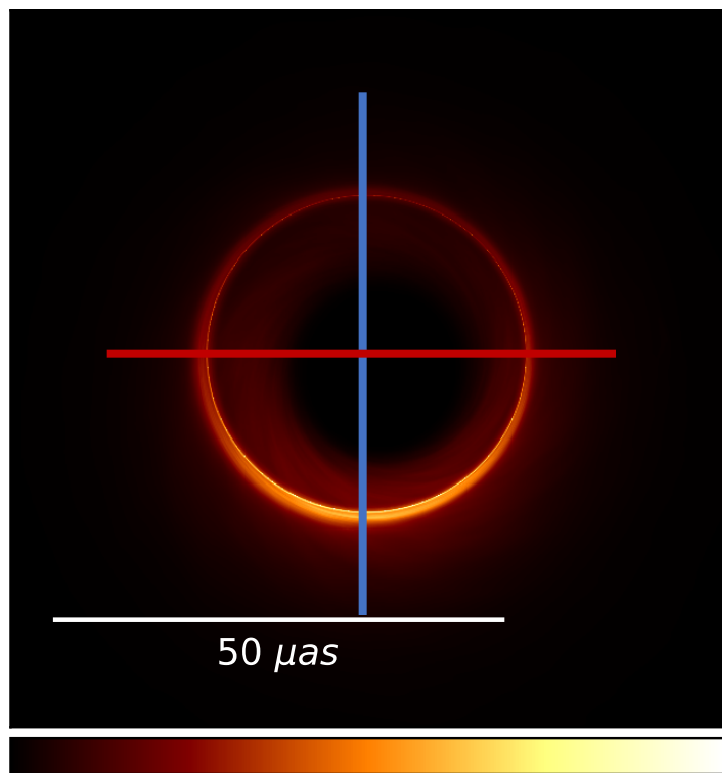
- We consider a toy model of emission ring at the deepest stagnation regions



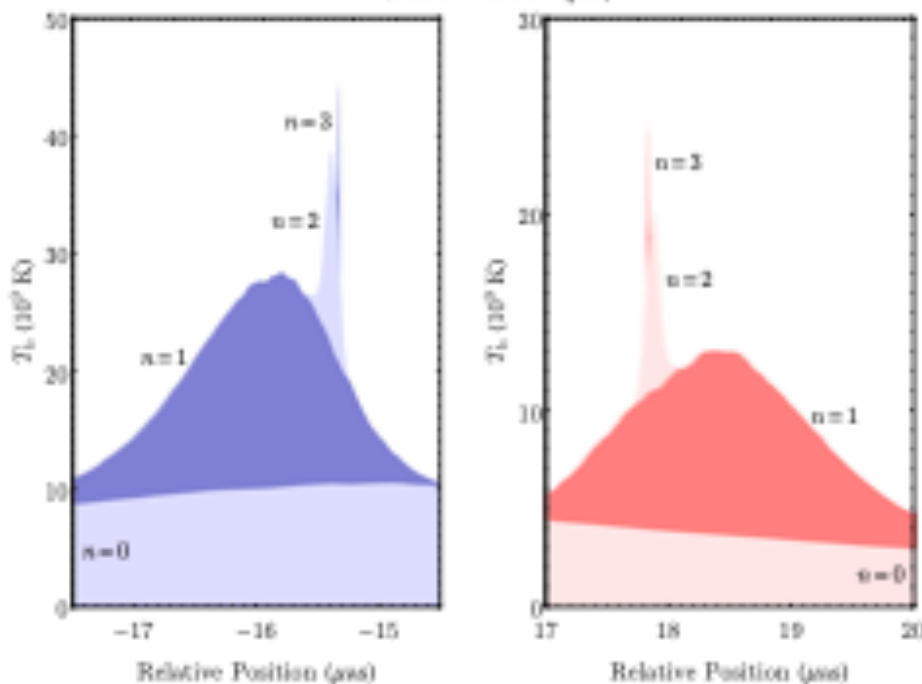
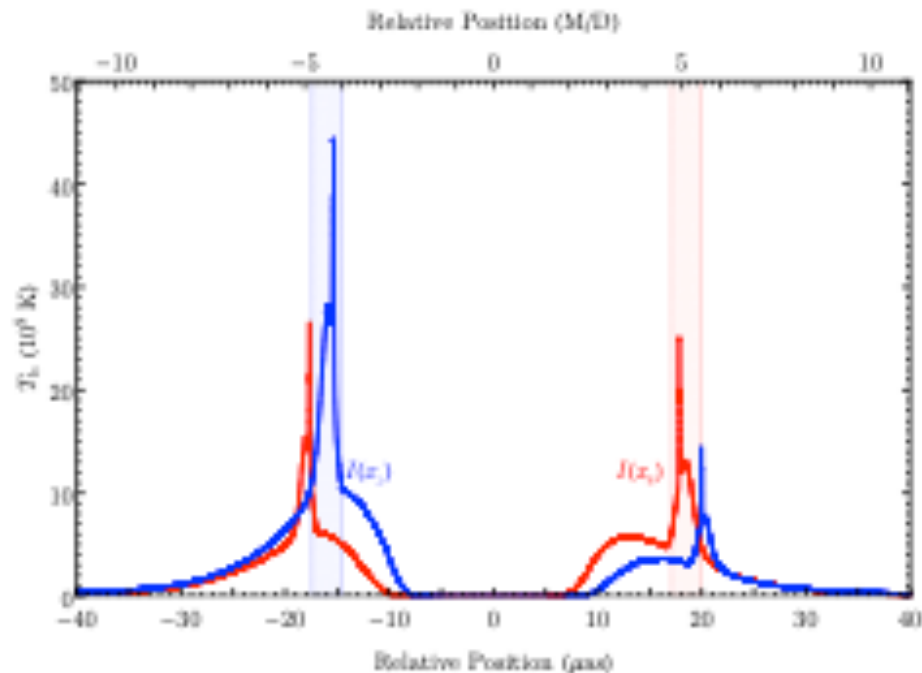
- Clear photon ring is observed more easily in the case of diffuse, non-localized emission
- The simple model indicates the ring at approaching jet appears to be too bright

Kawashima+ in prep.

Photon ring



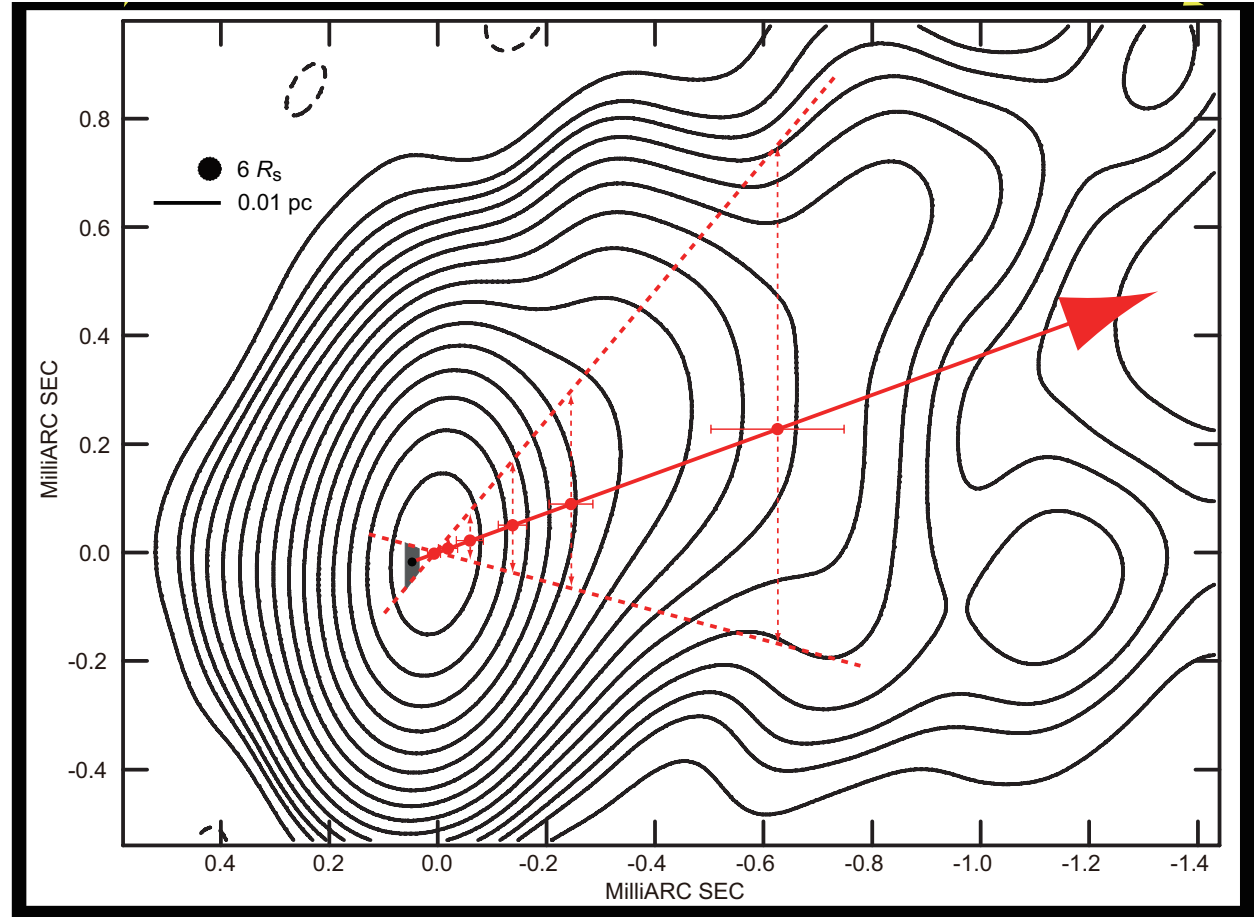
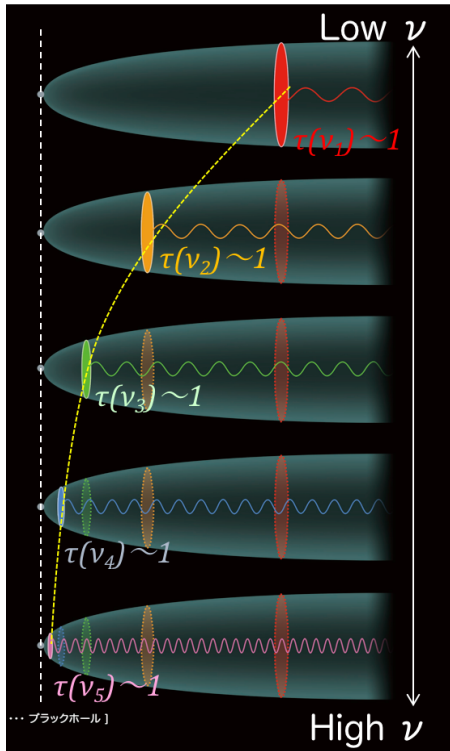
$a = 0.94$, $R_{\text{high}} = 10$, MAD



Number n of half-orbits

M87 jet observations (*activated by East-Asia researchers*)

VLBA 7mm



- High-accuracy core-shift measurement suggests the central engine resides very close to 7mm core

BHs with largest angular sizes

<i>Object</i>	M_{BH} ($10^8 M_{sun}$)	d (Mpc)	$1Rs$ (μas)
<i>SgrA*</i>	<i>0.04</i>	<i>0.008</i>	<i>10</i>
<i>M87</i>	<i>60</i> <small>(30?) Stellar dynamics (gas dynamics)</small>	<i>16.7</i>	<i>7</i>
<i>Sombrero</i>	<i>10</i>	<i>9.0</i>	<i>2.2</i>
<i>M84</i>	<i>8.5</i>	<i>17</i>	<i>1</i>
<i>Cen A</i>	<i>0.5</i>	<i>3.8</i>	<i>0.3</i>

($= 2r_g = 2GM/c^2$)

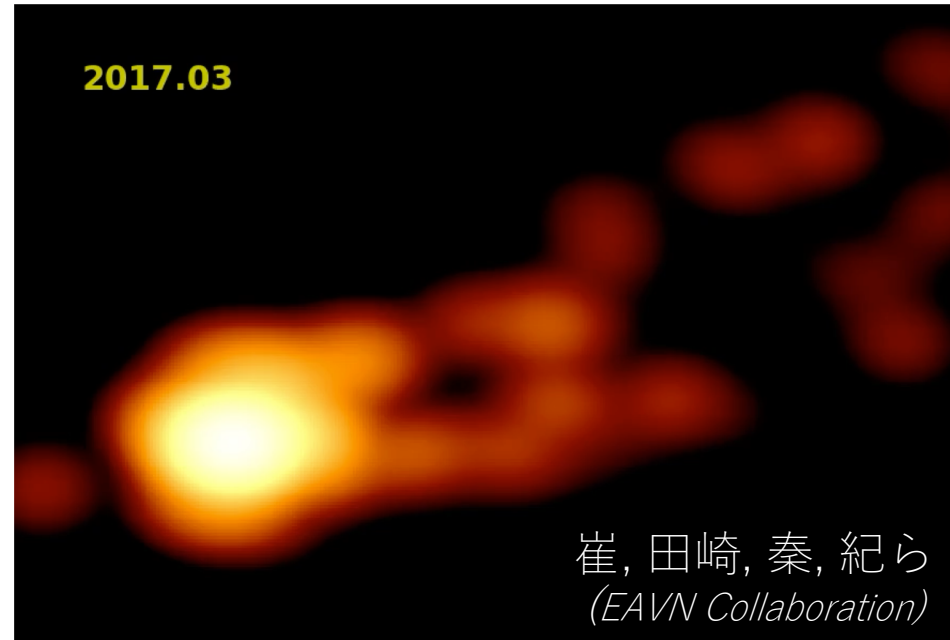
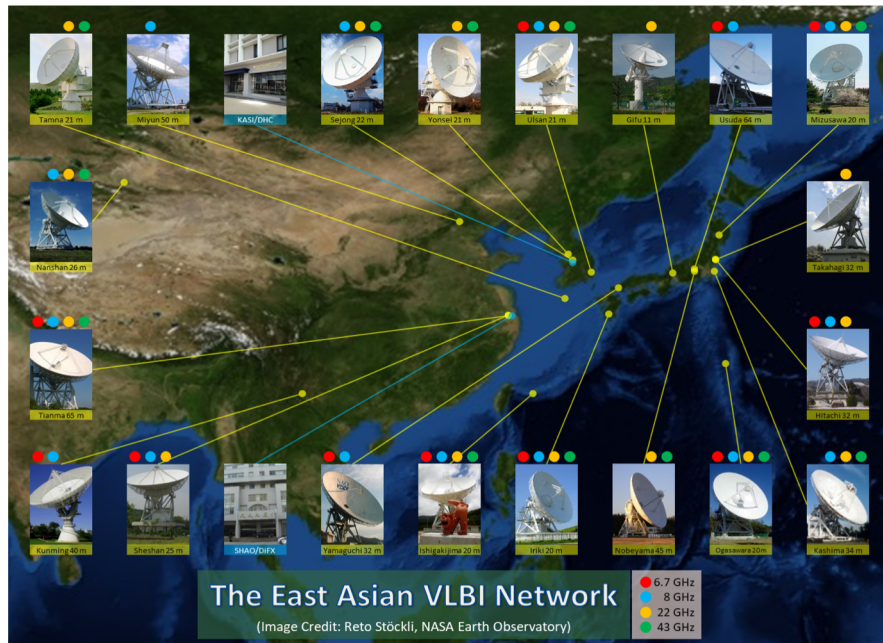
Summary & Discussion

- Radiative effects: GRMHD vs radiation GRMHD
- Non-thermal electrons
- Analysis limitations
 - Fast light approximation
 - Untilted disks
 - Pair production
 - Floors
- Alternatives to Kerr BHs

Ongoing & future works

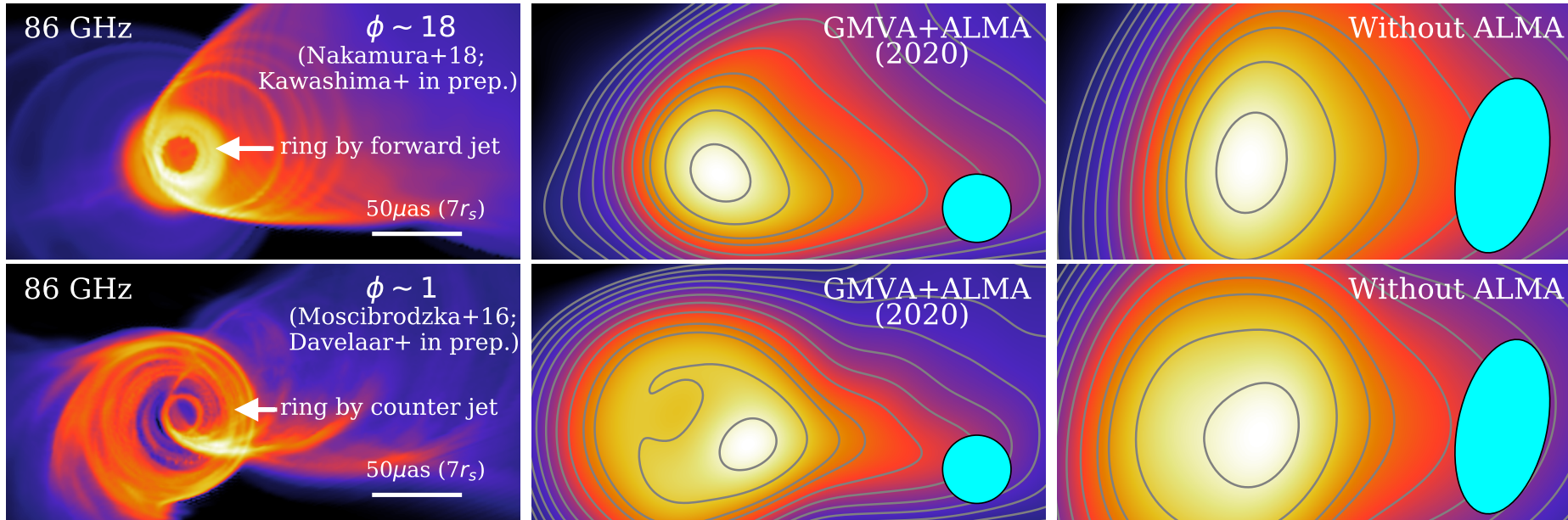
- Polarization: further constraints on n_e , B
 - Need parameter survey
- Combination of EHT data and lower freq. VLBI data
(Nakamura+18; Chael+19; Kino+14, 15; K. Takahashi+18)
- EHT 2020: more stations
 - imaging extended component
 - time variability?
- Future EHT 345 GHz campaigns
 - Green Land Telescope developed by ASIAA, Taiwan
 - Lower optical depth & higher spatial resolution
- -> Kawashima+2019; Nakamura+2019 in prep.

EHT data + EAVN data



- High cadence observations of M87/SgrA*
- Data quality comparable to VLBA
- 22/43 GHz → spectral index

GMVA + ALMA 2020 forecast



- EHT Collaboration, ALMA Cycle 7 + GMVA Proposal
- GMVA = Europe telescopes + VLBA & more [at 86 GHz]
- Asymmetric approaching-jet & bright counter-jet emission in the small ϕ model

The first EHT results: 6 ApJ Letters

Paper I: The Shadow of the Supermassive Black Hole (Summary Paper)

Coordinators: G. Bower, H. Falke & D. Psaltis

Paper II: Array and Instrumentation

Coordinators: S. Doeleman, V. Fish & R. Tilanus

Paper III: Data Processing and Calibration

Coordinators: L. Blackburn, S. Issaoun & M. Wielgus

Paper IV: Imaging of the Central Black Hole in M87

Coordinators: K. Akiyama, K. Bouman, A. Chael, J. Gomez & M. Johnson

Paper V: Physical Origin of the Asymmetric Ring

Coordinators: C. Gammie, Y. Mizuno & H.-Y. Pu

Paper VI: The Shadow and Mass of the Central Black Hole

Coordinators: K. Asada, A. Broderick, J. Dexter & F. Ozel

Event Horizon Telescope

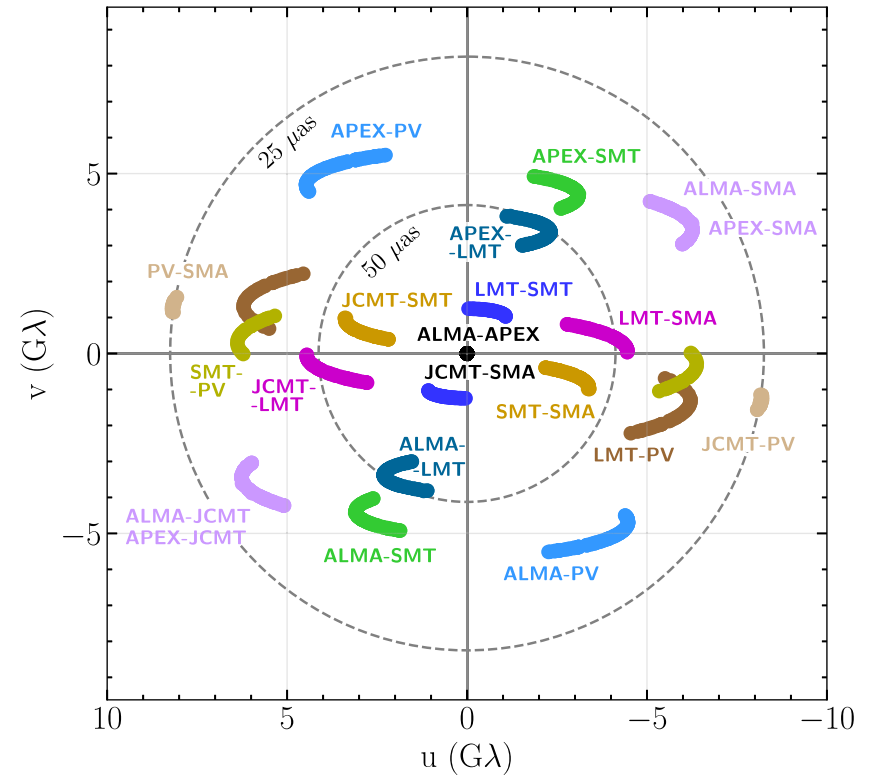
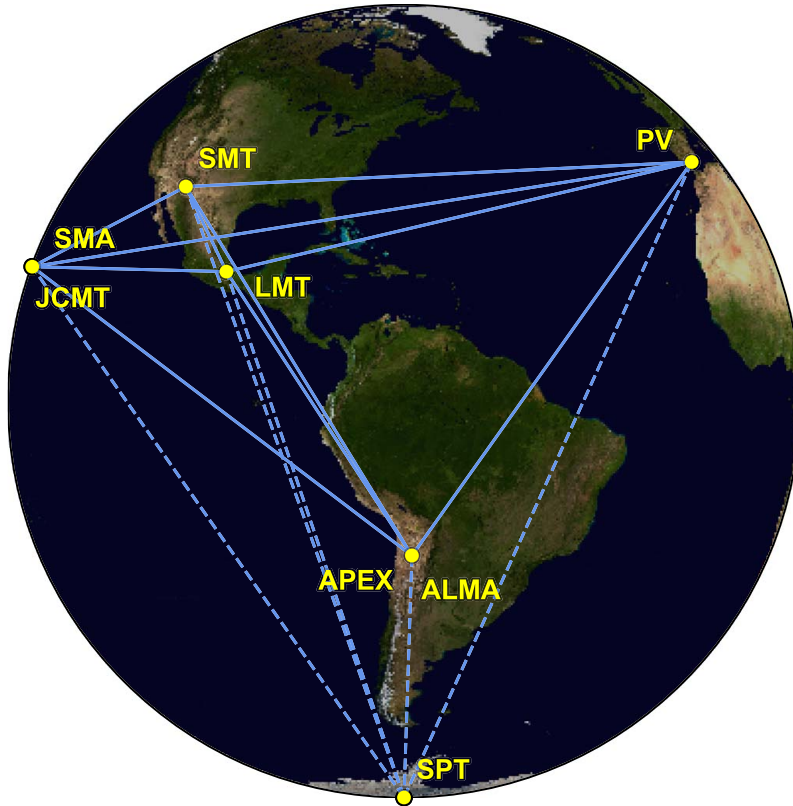
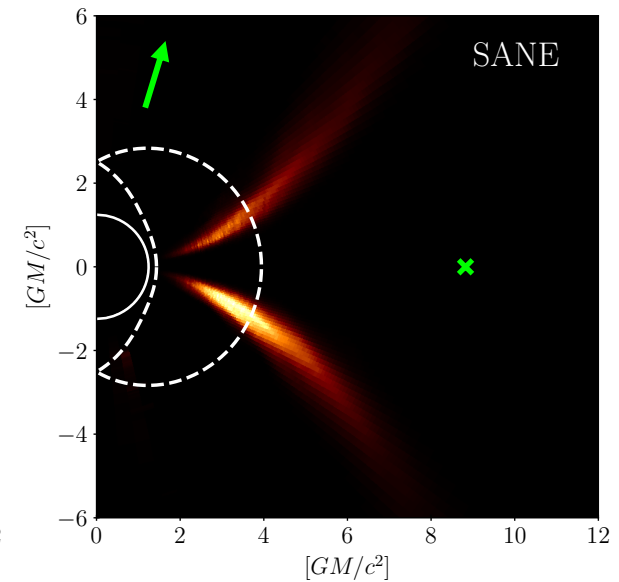
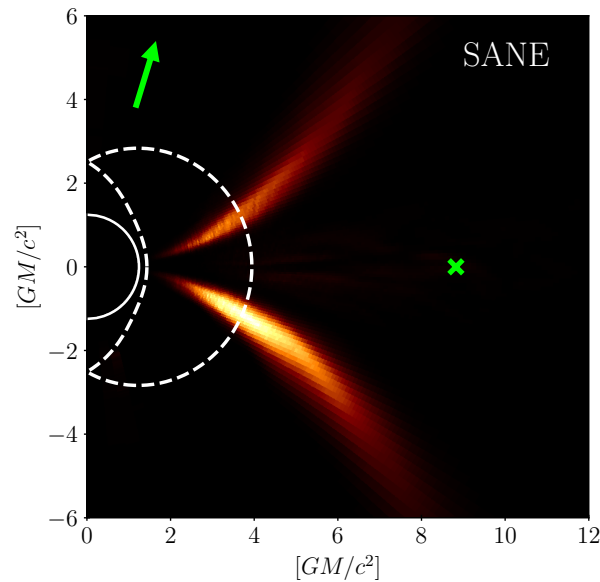
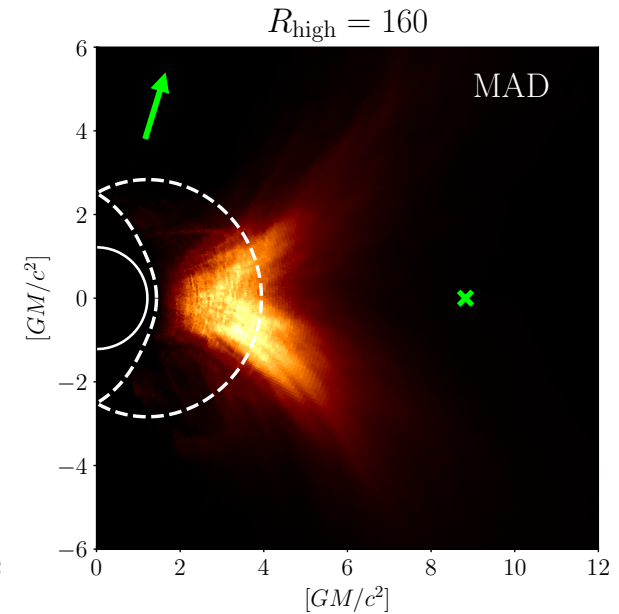
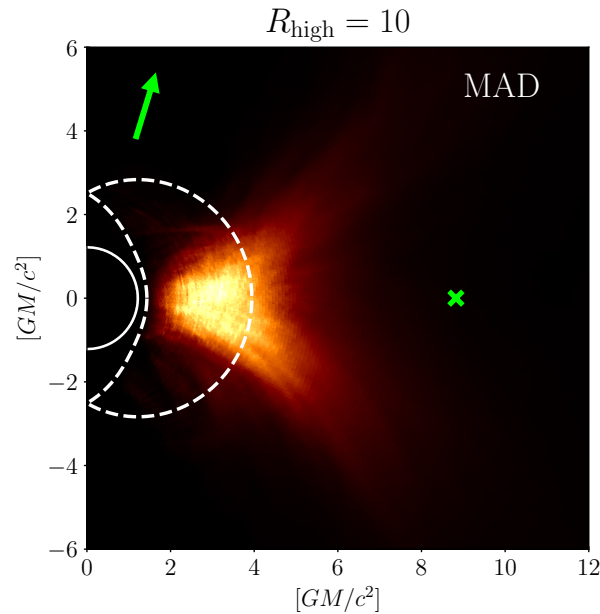


Figure 1. Eight stations of the EHT 2017 campaign over six geographic locations as viewed from the equatorial plane. Solid baselines represent mutual visibility on M87* (+12° declination). The dashed baselines were used for the calibration source 3C279 (see Papers [III](#) and [IV](#)).

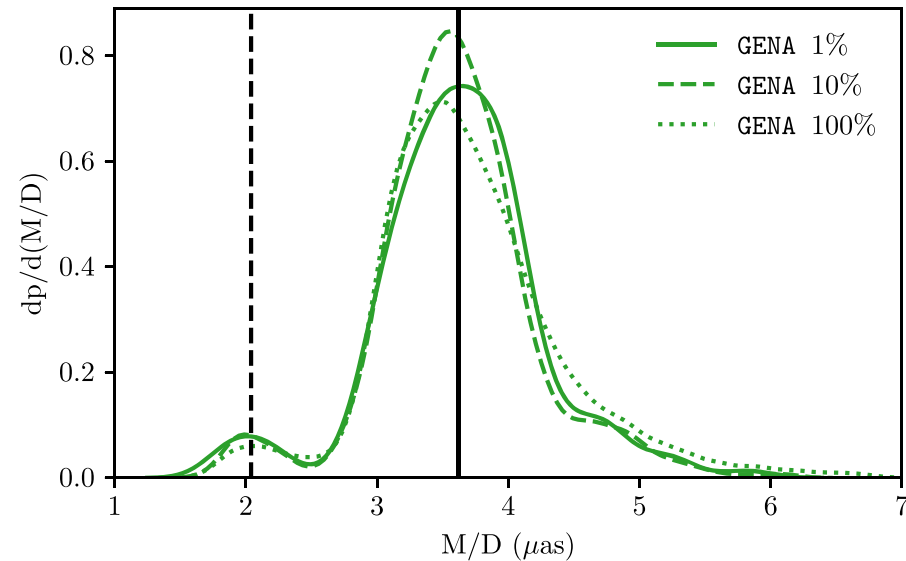
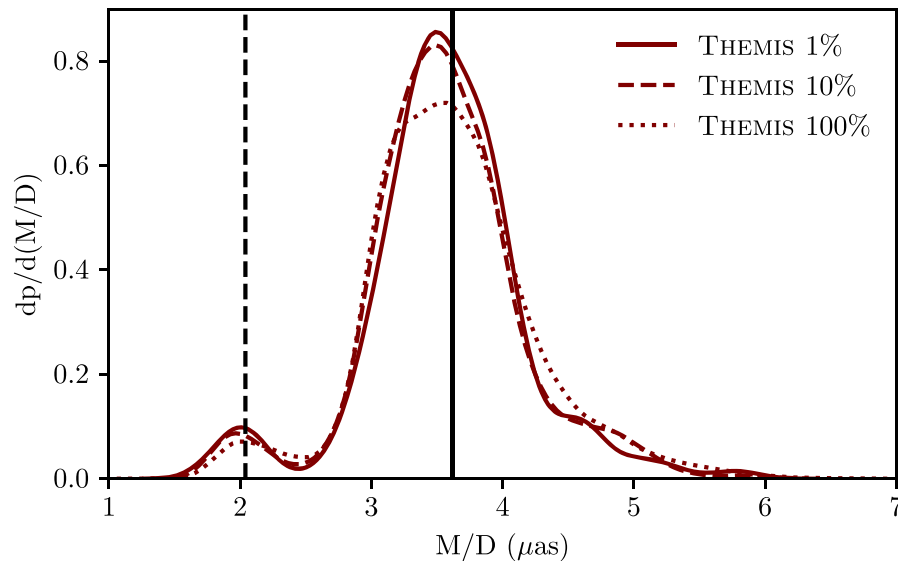
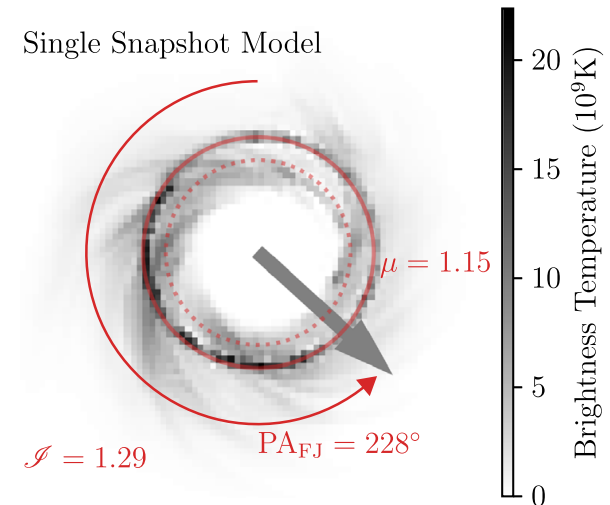
- Angular resolution $\theta \sim 1.3 \text{ mm}/10^4 \text{ km} \sim 25 \mu\text{as}$

- Retrograde models: $a_* < 0$
- ISCO radius is much larger
- MAD funnel widths are similar in pro- and retro-grade cases
(cf. Tchekhovskoy & McKinney 2012)
- Even in SANE models, funnel is wide



Model fitting

- Probability distribution of parameters M/D , C , and PA via MCMC method
- Each simulation code derive similar distribution

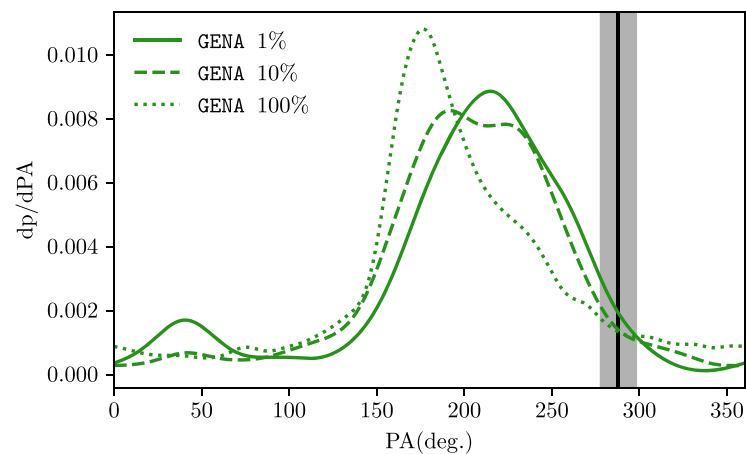
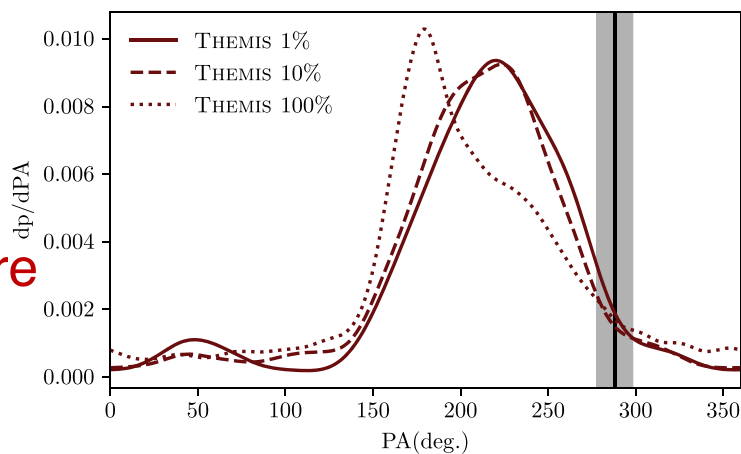


- $M \sim 6.5^{+0.7}_{-0.6} \times 10^9 M_{\text{sun}}$ (derived in paper VI)
- Consistent with the previous estimates based on stellar dynamics
- Small bump: $a^* < 0$, SANE, $R_{\text{high}} = 1$, rejected by jet luminosity

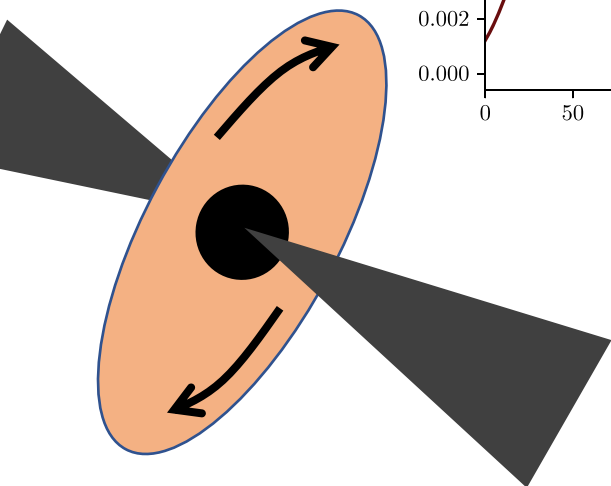
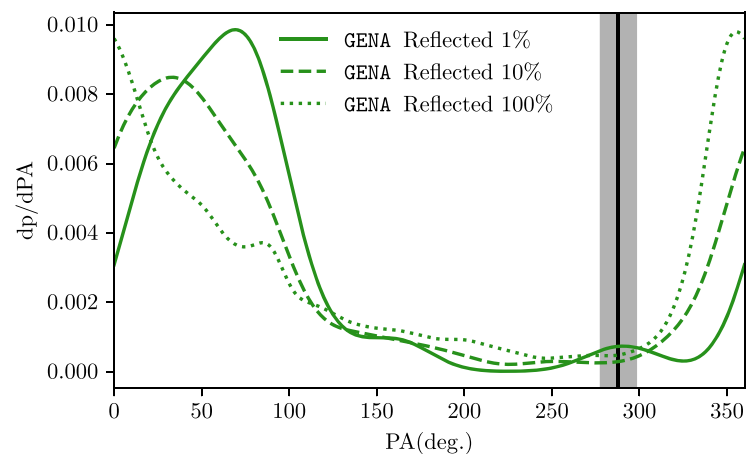
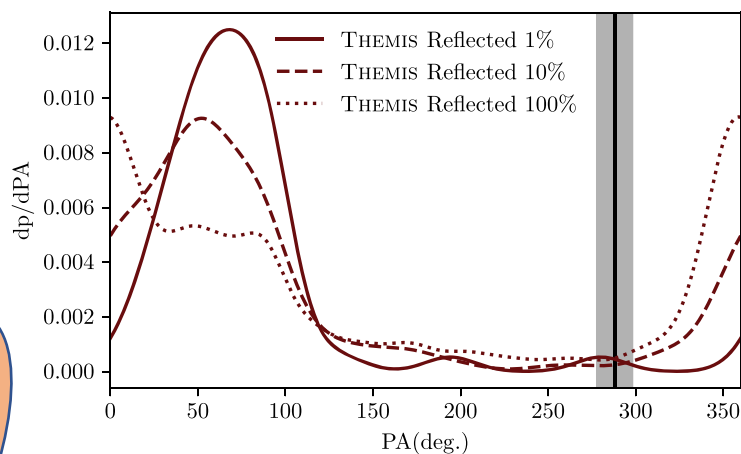
Large-scale jet orientation $PA \sim 288^\circ$

$i < 90^\circ, a_* < 0$
 $i > 90^\circ, a_* > 0$

These cases are
more likely

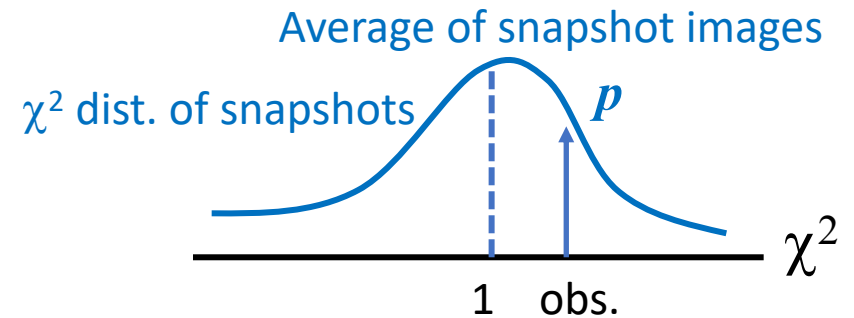
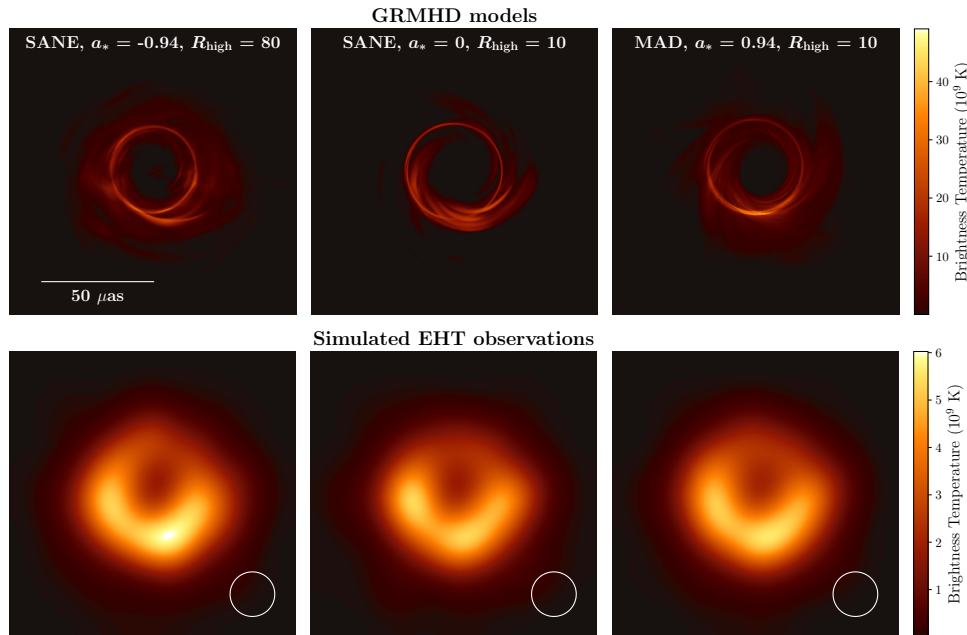


$i < 90^\circ, a_* > 0$
 $i > 90^\circ, a_* < 0$



Average Image Scoring^a Summary

Flux ^b	a_* ^c	$\langle p \rangle$ ^d	N_{model} ^e	MIN(p) ^f	MAX(p) ^g
SANE	-0.94	0.33	24	0.01	0.88
SANE	-0.5	0.19	24	0.01	0.73
SANE	0	0.23	24	0.01	0.92
SANE	0.5	0.51	30	0.02	0.97
SANE	0.75	0.74	6	0.48	0.98
SANE	0.88	0.65	6	0.26	0.94
SANE	0.94	0.49	24	0.01	0.92
SANE	0.97	0.12	6	0.06	0.40
MAD	-0.94	0.01	18	0.01	0.04
MAD	-0.5	0.75	18	0.34	0.98
MAD	0	0.22	18	0.01	0.62
MAD	0.5	0.17	18	0.02	0.54
MAD	0.75	0.28	18	0.01	0.72
MAD	0.94	0.21	18	0.02	0.50



- Overall, the observed image is consistent with expectations for the shadow of a Kerr BHs predicted by general relativity
- So many models are acceptable. This is likely because the source structure is dominated by the photon ring
- If the BH spin and M87's large scale jet are aligned, then the BH spine vector is pointed away from Earth

イベント・ホライズン・テレスコープ (EHT)

— 各地の電波望遠鏡をつなぎ、地球サイズの仮想望遠鏡を構成 —

2018年の観測

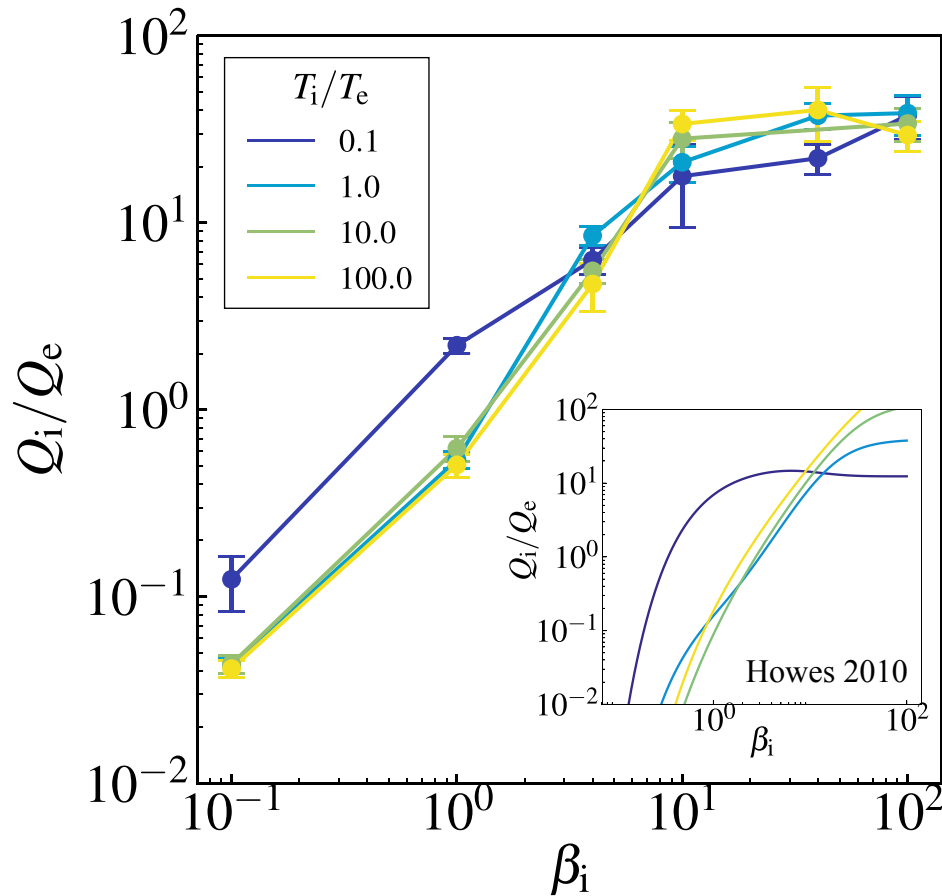


ALMA		アルマ望遠鏡 チリ・アタカマ砂漠
APEX		APEX チリ・アタカマ砂漠
30-M		IRAM 30m望遠鏡 スペイン・ピコベレタ
JCMT		ジェームズ・クラーク・マクスウェル望遠鏡 ハワイ・マウナケア
LMT		大型ミリ波望遠鏡 メキシコ・シエラネグラ
SMA		サブミリ波干渉計 ハワイ・マウナケア
SMT		サブミリ波望遠鏡 アリゾナ・グラハム山
SPT		南極点望遠鏡 南極点基地
GLT		グリーンランド望遠鏡 デンマーク・グリーンランド チュール空軍基地
Kitt Peak		キットピーク12m望遠鏡 アリゾナ・キットピーク
NOEMA		NOEMA観測所 フランス・プラトーデビュール

2020年に参加

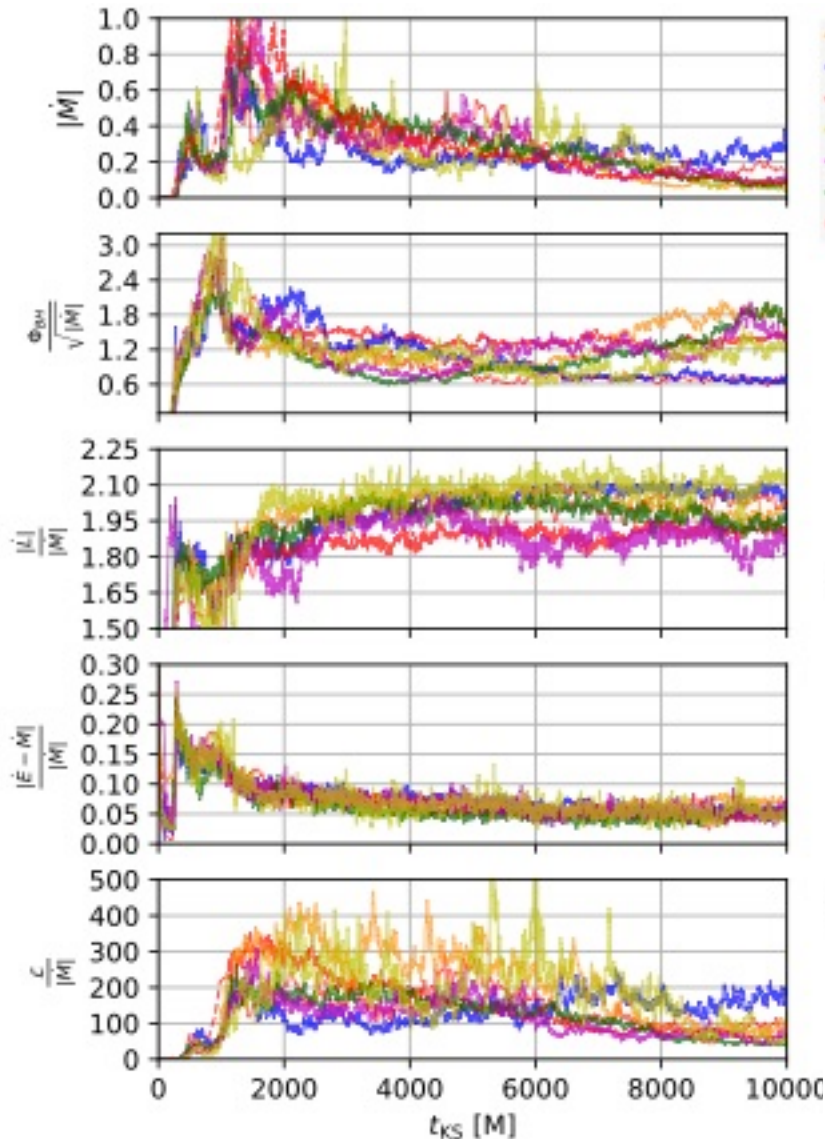


Turbulence cascade

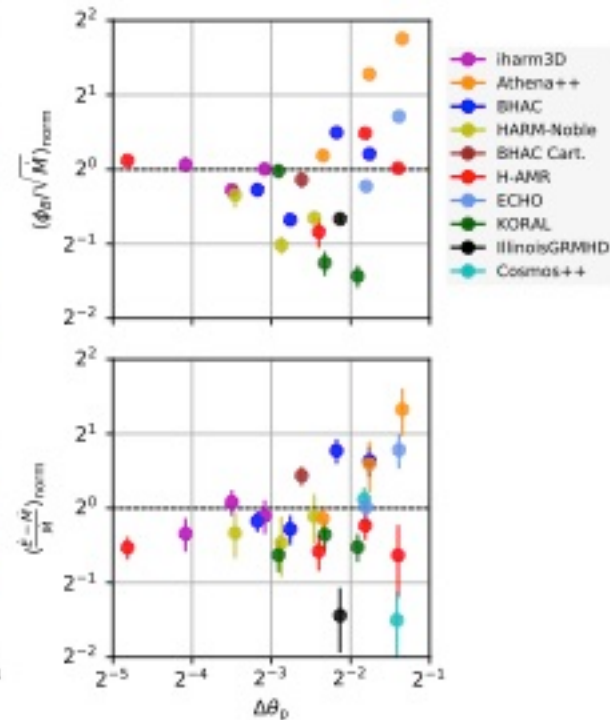
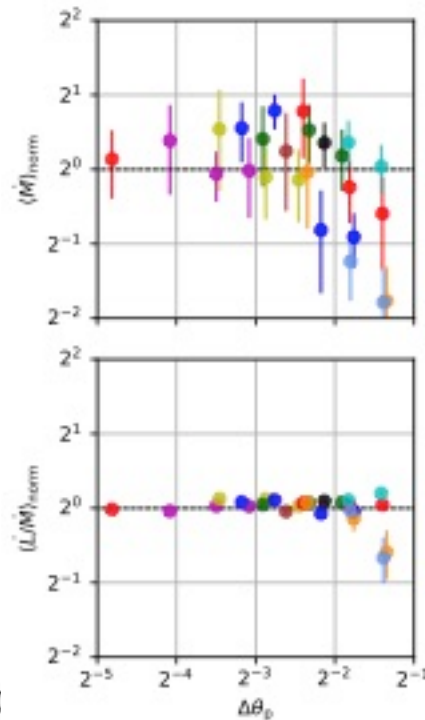


- Alfvén turbulent cascade
- MHD inertial range
→ ion Larmor scale
(conversion to ion heating)
→ kinetic Alfvén waves
(ultimately heating electrons)
- For low beta, ion thermal speed \ll Alfvén speed, so that ions cannot interact with Alfvénic perturbations

GRMHD code comparison



- Parameter fitting results for M87 are consistent in different codes



Polarization

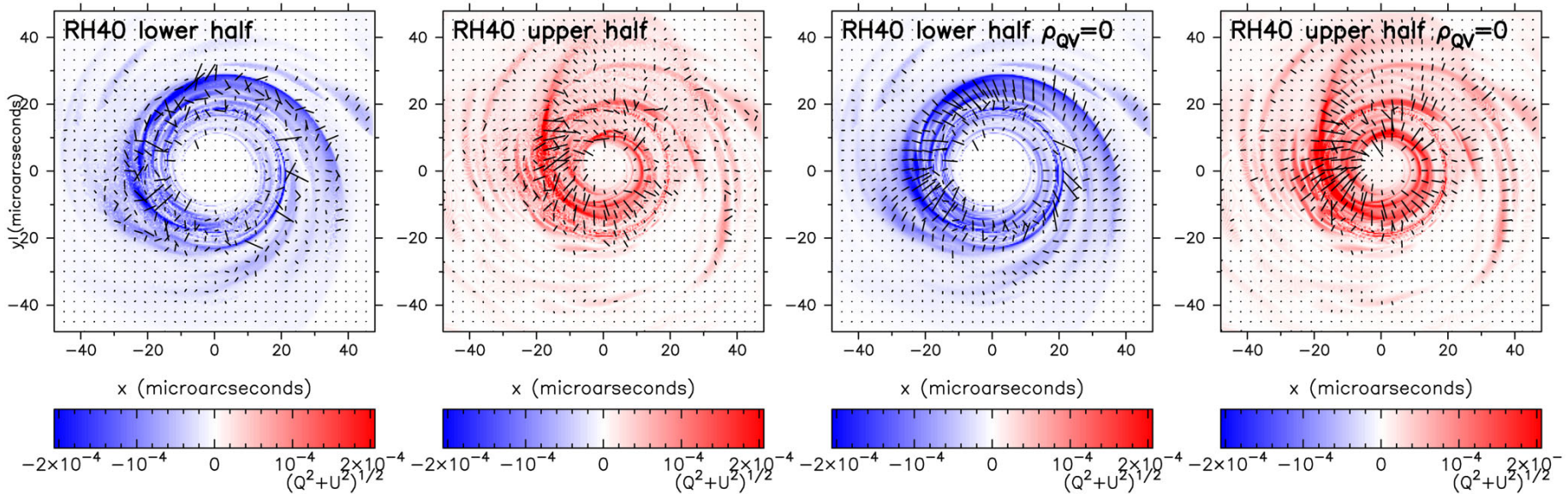
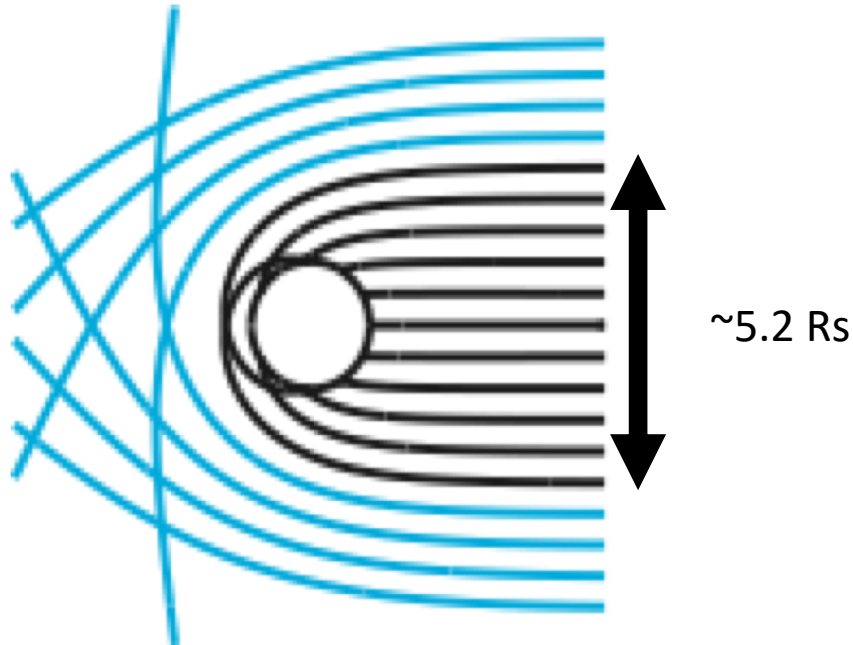


Figure 5. First and second panels: polarized emission $\sqrt{Q^2 + U^2}$ for each pixel originating from below (blue) and above (red) the mid-plane together with polarization ticks for model RH40. Third and fourth panels: same as first and second panels but with Faraday effects switched off. The model without Faraday effects shows coherent polarization signals from both counter and forward jets.

counter jet and forward jet. In Fig. 5, the counter-jet polarization (first panel) is evidently significantly scrambled compared to the coherent signal from the forward jet (second panel). The total LP degree from the counter jet is 1 per cent. This is smaller than the total polarization degree of the forward jet which is 3.1 per cent.

Black Hole Shadow

Non-spinning Black Hole



Maximumly Rotating Black Hole

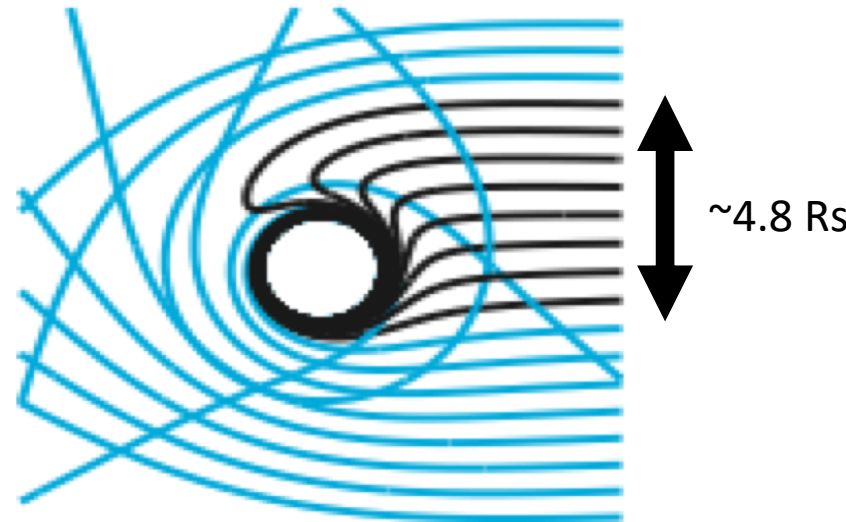
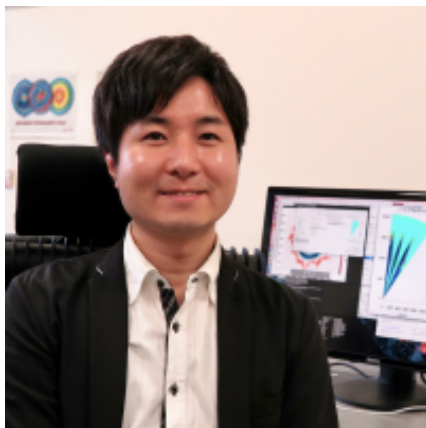
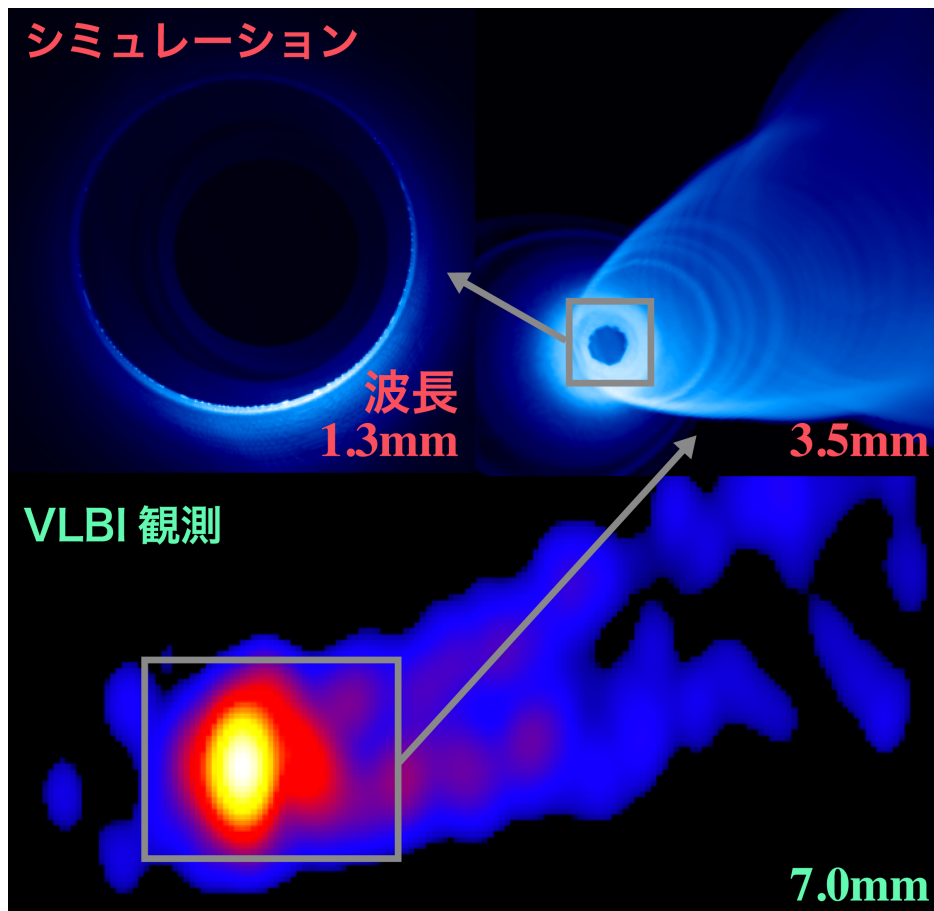


Figure credit: H.-Y. Pu

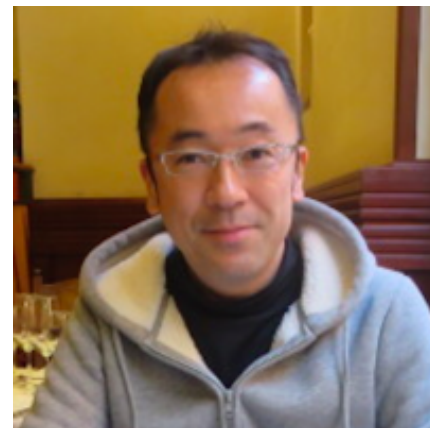
Participants to Paper V from East Asia region



T. Kawashima
(NAOJ)



We will connect jet-ring!



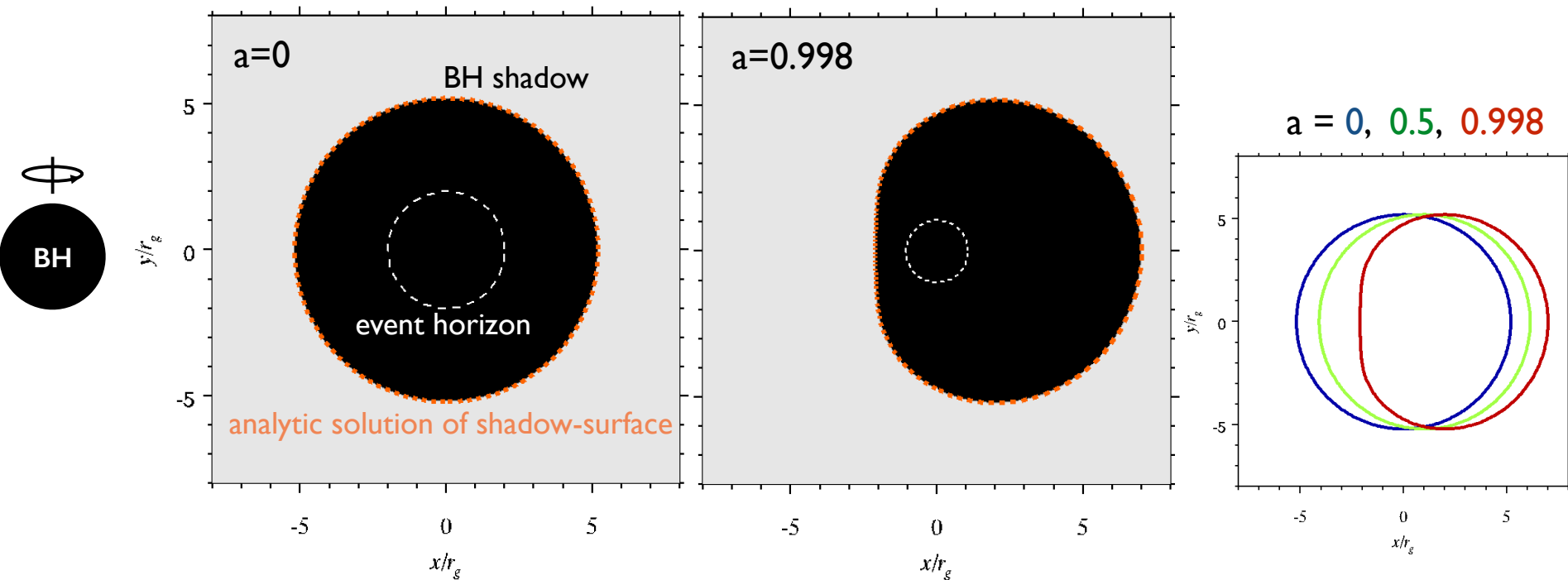
M. Kino
(NAOJ/Kogakuin)



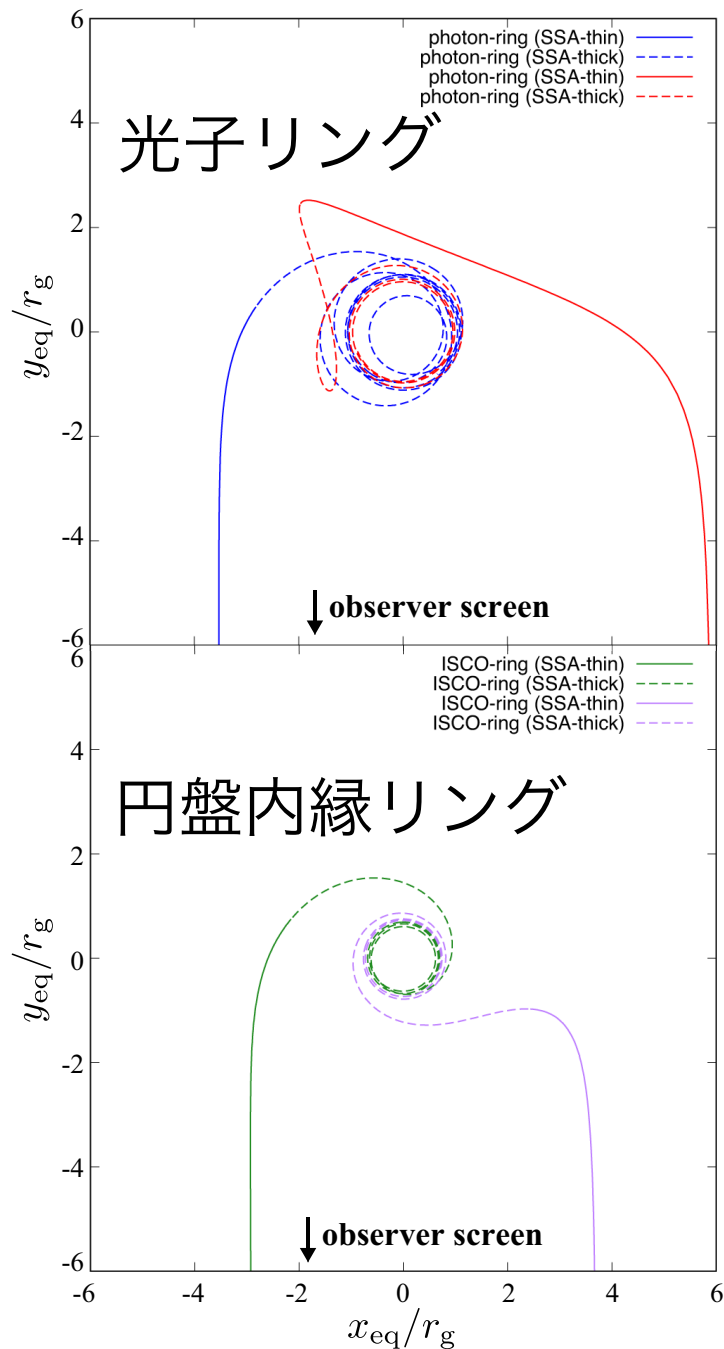
K. Toma
(Tohoku)



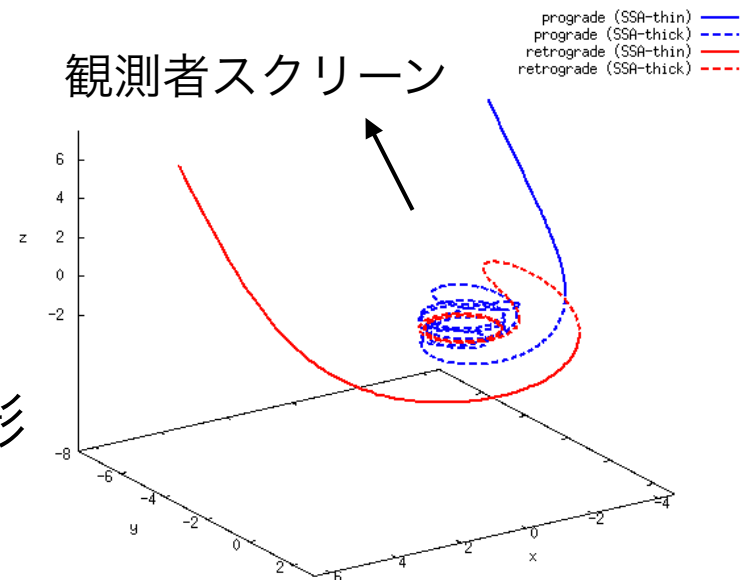
M. Nakamura
(ASIAA)



- BH質量依存性：光子リング(BHシャドウ)のサイズはBH質量に比例。
- BHスピン依存性：サイズはわずか約 $\pm 5\%$ のずれ。
光子リング(シャドウ)の位置がスピン軸に垂直方向にずれるのみ。
- BH質量を決めるのには適している。一方でスピンを決めるのは困難。



赤道面に射影



- 光子リングは大きさはスピンに依存しないが、位置はスピンに依存(横にシフト)。
- これは光子球軌道はスピンに対して順回転、逆回転で大きく半径が変わるため。
- 円盤内縁リングを形成する光子は光子球に乗る必要がないので角運動量の正負にあまり依存しない。

Image models

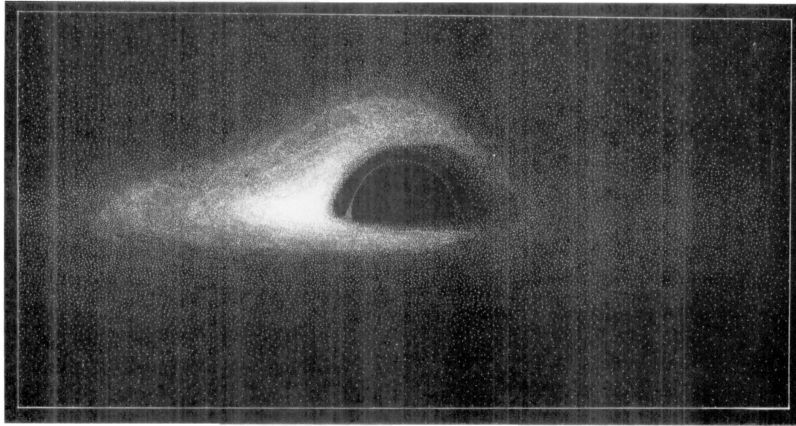


Fig. 11. Simulated photograph of a spherical black hole with thin accretion disk

- Standard disk model
Luminet 1979; Bardeen 1973

- RIAF + jet models (GRMHD simulations + GRRT calculations)
Falke, Melia & Agol 2000; Dexter+2012; Moscibrozka+2016

